Mon. Not. R. Astron. Soc. **000**, 000–000 (0000) Printed 1 February 2008 (MN LATEX style file v1.4)

On the effects of dynamical evolution on the initial mass function of globular clusters

E.Vesperini⋆, D.C.Heggie†

Department of Mathematics and Statistics, University of Edinburgh, King's Buildings, Edinburgh, EH9 3JZ

1 February 2008

ABSTRACT

In this paper we show the results of a large set of N-body simulations modelling the evolution of globular clusters driven by relaxation, stellar evolution, disk shocking and including the effects of the tidal field of the Galaxy. We investigate the evolution of multi-mass models with a power-law initial mass function (IMF) starting with different initial masses, concentrations, slopes of the IMF and located at different galactocentric distances. We show to what extent the effects of the various evolutionary processes alter the shape of the IMF and to what extent these changes depend on the position of the cluster in the Galaxy. Both the changes in the global mass function and in the local one (measured at different distances from the cluster center) are investigated showing whether and where the local mass function keeps memory of the IMF and where it provides a good indication of the current global mass function.

The evolution of the population of white dwarfs is also followed in detail and we supply an estimate of the fraction of the current value of the total mass expected to be in white dwarfs depending on the main initial conditions for the cluster (mass and position in the Galaxy). Simple analytical expression by which it is possible to calculate the main quantities of interest (total mass, fraction of white dwarfs, slope of the mass function) at any time t for a larger number of different initial conditions than those investigated numerically have been derived.

Key words: globular clusters:general – stellar dynamics

1 INTRODUCTION

Investigation of the mass function of globular clusters is of great importance for a variety of problems in astrophysics covering star formation processes, the dynamical evolution of stellar systems and the nature of dark matter in the Galaxy. Large progress has been made in recent years both by ground based observation and, more recently, thanks to observations by HST. Nevertheless most of issues concerning the shape of the initial mass function (IMF), its dependence on cluster parameters, the actual relevance of dynamical processes in its evolution and the relation between the IMF and the present-day mass function (PDMF) are still matters of debate.

The first investigation addressing the dependence of the slope of the mass function on cluster structural parameters and metallicity was carried out by McClure et al. (1986) who found the slope of the PDMF for a sample of six galactic clusters to be correlated with their metallicity, the low-metallicity clusters having steeper mass functions. In subsequent work Capaccioli, Ortolani & Piotto (1991), Piotto (1991) and Capaccioli, Piotto & Stiavelli (1993) have considered a larger sample of clusters and have questioned the conclusion of McClure et al. and showed the correlation between the slope of the PDMF and the position of the cluster in the Galaxy to be stronger than that with the metallicity. Finally Djorgovski, Piotto & Capaccioli (1993) have addressed this problem again by multivariate statistical methods and have concluded that both the position in the Galaxy (galactocentric distance and height above the disk) and the metallicity play some role in determining the slope of

⋆ Present address: Department of Physics and Astronomy, University of Massachusetts, Amherst, MA 01003-4525, USA; E-mail:vesperin@falcon.phast.umass.edu

† E-mail:d.c.heggie@ed.ac.uk

the PDMF but the former is more important than the latter. The observed correlation is in the sense of clusters more distant from the galactic center or from the disk having steeper mass functions.

The data used in the above works are from ground based observations and the slopes are measured for a limited range of star masses ($0.5 < m/m_{\odot} < 0.8$). Recent investigations of the luminosity function of some galactic globular clusters by HST have been able to extend the available data to fainter magnitudes (Paresce, Demarchi & Romaniello 1995, De Marchi & Paresce 1995ab, Elson et al. 1995, Piotto, Cool & King 1996,1997, Santiago, Elson & Gilmore 1996). HST data for for 47 Tuc , ωCen , NGC 6397, M15 and M30 are now available. These clusters span a wide range of values of metallicity, their structural parameters suggest they have undergone a very different dynamical evolution and the issue concerning the origin of the shape of the PDMF has been addressed again in the light of this new data.

De Marchi & Paresce (1995b) compare the MF of NGC 6397, M15 and 47 Tuc showing that all these clusters have a flat MF for low-masses; they point out that the MF is flat at the low-mass end for both NGC 6397 and M15 and that these MFs are very similar though these clusters are likely to have had a different dynamical history. As for 47 Tuc , this is shown to have a different MF from M15 and NGC 6397. Noting that the metallicity of 47 Tuc is very different from that of NGC 6397 and M15 De Marchi & Paresce make the hypothesis that the differences between the MFs of these clusters might be due to a different initial mass function (IMF) depending on the metallicity, thus giving new support to the conclusion of McClure et al. (1986), with the subsequent dynamical evolution playing no relevant role.

However in a recent work, Santiago et al. (1996) show that the MF of ωCen , whose metallicity is similar to that of 47 Tuc , is steeper than the MF of 47 Tuc , and cast some doubt on the scenario supported by De Marchi and Paresce. Santiago et al. point out that if one assumes a universal IMF, the comparison of the MF of ωCen with those of NGC 6397, M15, 47 Tuc would indicate that the latter clusters have experienced significant dynamical evolution with strong depletion of low-mass stars. Finally Piotto et al. (1996,1997) argue that the reason why De Marchi and Paresce get a similar MF for NGC 6397 and M15 is that they compare only the low-mass end and show that, by comparing the LF including the data for the bright end, NGC 6397 appears to be markedly deficient in faint stars. As the metallicities of NGC 6397 and M15 are very similar, this result lends strong support to the hypothesis that the MF of NGC 6397 is flattened by dynamical processes. King (1996) notes that this hypothesis is further enforced by the comparison of the orbits of NGC 6397 and M15, as obtained by Dauphole et al. (1996); according to this work NGC 6397 would be more affected by the tidal interaction with the Galaxy as it would cross the disk more frequently and would have a smaller perigalactic distance than M15.

Additional observations covering a larger range of cluster parameters are necessary, as well as theoretical investigations addressing both the problems connected with the stellar evolution models (see Alexander et al. 1997, D'Antona & Mazzitelli 1996 for two recent works in this direction) allowing a better determination of the mass-luminosity relationship for low-mass low-metallicity stars (see e.g. Elson et al. 1995 for a clear presentation of the problems due to the uncertainties on $M-L$ relation) and those connected with the dynamical evolution, thus clarifying the efficiency of evolutionary processes in modifying the IMF.

As for this latter aspect the situation is far from being clear: simple semi-analytical models by Stiavelli et al. (1991), Stiavelli, Piotto & Capaccioli (1992) and Capaccioli et al. (1993) suggest that disk shocking could play a relevant role in establishing the observed correlation between the slope of the PDMF and the position in the Galaxy and some indications on the role of evaporation due to two-body relaxation come from many multi-mass Fokker-Planck investigations of the dynamical evolution of clusters (see e.g. Chernoff & Weinberg 1990, Weinberg 1994) but no firm conclusion has been reached on the relevance of various dynamical processes in giving rise to the observed correlation between the slope of the mass function and position in the Galaxy and the interplay between different dynamical processes has not been fully explored.

In this paper we show the results of a set of N- body simulations including the effects of the presence of the tidal field of the Galaxy, stellar evolution, disk shocking, two-body relaxation and spanning a range of different initial conditions for the mass and concentration of the cluster, the slope of the IMF and the distance from the galactic center.

The main goal of our theoretical investigation is that of assessing the importance of various evolutionary processes in altering the mass function of a globular cluster, trying to establish to what extent these processes can be responsible for the differences observed between the MFs in galactic globular clusters. Having included the effects of stellar evolution in our investigation we will be able to address some other issues concerning the evolution of the stellar content of globular clusters. In particular we will focus our attention on the fraction of white dwarfs expected to be present in a cluster during the different stages of its dynamical evolution. These are of increasing interest for a variety of reasons. It had long been realised that white dwarfs should exist in some abundance in globular clusters, and they have been included routinely in dynamical models. Otherwise, however, little attention was paid to them while they remained unobservable. That situation has changed dramatically in recent years (e.g. Richer et al. 1995), and it is now claimed that white dwarfs formed up to 9 Gyr ago have been detected (Richer et al. 1997). Furthermore recent suggestions have been made that white dwarfs could account for as much as 50 percent of the total mass of some clusters (Heggie & Hut 1996) or up to 85 percent in some locations in other clusters (Gebhardt et al. 1997). This sudden burst of interest in white dwarfs will stimulate renewed attention in their influence on cluster dynamics, and has motivated the work reported in section 3.3.

In Sect.2 we describe the method used for our investigation. In Sect.3 the results of simulations including the effects

of stellar evolution and two-body relaxation only are described, and some analytical expressions are derived for the main quantities of interest for this work. In Sect.4 the results of runs including also the effects of disk shocking are described and, where possible, we generalize the analytical expressions obtained in sect.3 . The dependence of the results on the initial number of particles used in the simulations are discussed in sect.5. Summary and conclusions are in Sect.6.

2 METHOD

All the N-body simulations made for our investigation have been carried out using a version of the code NBODY4 (Aarseth 1985) including mass loss of single stars due to stellar evolution, the effects of disk shocking and of the tidal field of the Galaxy. The code is a direct summation code adopting an Hermite integration scheme and a binary hierarchy of time-steps; a GRAPE-4 board containing 48 HARP chips (Makino, Kokubo & Taiji 1993) connected to a Dec Alphastation 3000/700 has been used for the evaluation of the forces and force derivatives required by the Hermite scheme. Most of the simulations carried out in this work start with a total number of particles $N = 4096$ and it took a CPU time ranging from about 3 to 15 hours for each of them to be completed depending on the initial concentration of the system and its galactocentric distance (for further information on the code and the performance of the board see e.g. Aarseth 1994, Aarseth & Heggie 1997a).

In our simulations we have assumed the cluster to be on a circular orbit and to move in a Keplerian potential determined by a point mass M_g equal to the total mass of the Galaxy inside the adopted galactocentric distance R_g; the value of the circular speed has been taken equal to $v_c = 220$ km/s. If we denote the angular velocity of the cluster around the galaxy by ω and take the coordinates of a star relative to the center of the cluster with the x-axis pointing in the direction away from the galactic center and the y-axis in the direction of the cluster motion we can write the equations of motion for a star in the cluster as (see e.g. Chandrasekhar 1942)

$$\begin{aligned} &\frac{d^2x}{dt^2} - 2\omega\frac{dy}{dt} - 3\omega^2 x = F_x \\ &\frac{d^2y}{dt^2} + 2\omega\frac{dx}{dt} = F_y \\ &\frac{d^2z}{dt^2} + \omega^2 z = F_z \end{aligned} \tag{1}$$

where $\mathbf{F}$ represent the acceleration from other stars in the cluster and the terms involving ω on the left-side of the equations are due to the Coriolis, centrifugal and tidal field accelerations.

King's models (King 1966) with different concentrations have been used to produce initial conditions and the standard N- body units (Heggie & Mathieu 1986) (total mass $M = 1$, $G = 1$ and initial energy equal to -1/4) have been adopted. The value of ω in N-body units is given by its initial relationship with the tidal radius (see Aarseth & Heggie 1997a)

$$r_t^* = (3\omega^{*2})^{-1/3}, \tag{2}$$

where the $*$ denotes quantities in N-body units.

Masses of stars have been assigned according to a power-law mass function

$$dN(m) = m^{-\alpha} dm$$

between $0.1 m_\odot$ and $15 m_\odot$ and initially there is no equipartition of energies of stars with different masses.

Disk shocking has been included according to the model described in Chernoff, Kochanek & Shapiro (1986). Following Spitzer (1958), Chernoff et al. describe the motion of a single star in the cluster as that of an harmonic oscillator with a frequency Ω perturbed by the force due to the disk. Assuming the orbit to be perpendicular to the plane of the disk and choosing the direction of motion along the y-axis, the equation of motion of a star in a frame at rest with respect to the center of the cluster is

$$\frac{\mathrm{d}^2\delta y}{\mathrm{d}t^2} + \Omega^2 \delta y = g(t)\delta y \tag{3}$$

where δy is the distance between the star and the center of the cluster, y the height of the center of the cluster over the disk and $g(t)$ is the differential acceleration due to the disk.

Modelling the disk as a one-component isothermal self-gravitating gas and assuming an exponential decay for the disk surface density, the acceleration due to the disk is given by

$$K_y = K_0 \tanh(y/y_0) \mathrm{e}^{-R_g/h}. \tag{4}$$

where R_g is the galactocentric distance and y_0 and h are the disk scale height and characteristic scale length respectively.

Starting from the above equations Chernoff et al. show that the change of velocity in the y direction suffered by a star due to the disk shocking can be written as

$$\Delta v_y = \delta y I_c(\Omega) \tag{5}$$

where I_c is

$$I_c = \frac{\pi\Omega}{2\nu^2 \sinh(\pi\Omega/2\nu)} \frac{K_0}{z_0} \mathrm{e}^{-R_g/h} \tag{6}$$

and $\nu = v_c/2y_0$ is the frequency of disk crossing. When $\nu \gg \Omega$, the above expression provides the same result which would be obtained in the impulse approximation (see e.g. Spitzer 1987) while for $\nu < \Omega$ the crossing is adiabatic and the change in star's velocity tends exponentially to zero. Notice that, in the pure impulse approximation, (as adopted, for example, by Capaccioli et al. (1993)), the effect of a disk shock is minimised by choosing an orbit which crosses the disk perpendicularly, as we have done, because then ν is maximised (for a given circular speed). The adiabatic correction, however, suppresses low-frequency disk shocking, and the net result is that the effect of disk shocking is almost independent of the inclination of the orbit over a wide range (Chernoff, Kochanek & Shapiro 1986).

In our investigation we have adopted the two-component disk model obtained by Chernoff et al. from fitting Bahcall's (1984) determination of acceleration in the solar neighbourhood

$$K_y(R_g = 8 \text{ Kpc}, y) = \sum_i K_{0i} \tanh(y/y_{0i}) \tag{7}$$

with

$$K_{01} = 3.47 \times 10^{-9} \text{cm s}^{-2};\ \ y_{01} = 175\text{pc}$$

$$K_{02} = 3.96 \times 10^{-9} \text{cm s}^{-2};\ \ y_{02} = 550\text{pc};$$

and the scale length has been taken equal to $h = 3.5$ Kpc (see e.g. Bahcall, Schmidt & Soneira 1982).

In the simulations including the effects of disk shocking, each half-orbital period of the cluster around the Galaxy the y-component of the velocities of all the stars in the system have been changed according to eq.(5) (where I_c has been replaced by the sum, $I_{c1} + I_{c2}$, with $I_{c1,2}$ being the function I_c evaluated for the two disk components) with the frequency Ω taken to be equal to the ratio of the current value of tangential velocity of the star to its radial distance from the cluster center.

Stellar evolution has been modelled by assuming that the mass lost by each star immediately escapes from the cluster (this is likely to be a reasonable approximation since the escape velocity from a typical globular cluster is of the order of 10 km s^{-1}) and thus the mass of each star has been decreased at the appropriate time by an amount depending on the initial value of the mass itself. The fraction of mass lost by stellar evolution and the time when mass loss has to take place in the simulation have been calculated adopting the same model used in Chernoff & Weinberg (1990) (see also Fukushige & Heggie 1995): stars whose initial mass is larger than 8 $m_\odot$ end their life as neutron stars with a mass equal to 1.4 $m_\odot$, stars with $4.7 < m/m_\odot < 8$ are assumed to leave no remnant and stars less massive than $4.7 m_\odot$ produce white dwarfs with a mass equal to $0.58 + 0.22(m/m_\odot - 1)$; the times the mass must be removed are determined by a linear interpolation of the main sequence times calculated by Iben & Renzini (1983) and reported in Table 1B of Chernoff & Weinberg (1990). We have assumed that there is no kick velocity from the supernova explosion for stars ending their evolution as neutron stars. Though consistent with the assumptions of Chernoff & Weinberg (1990) this assumption is very likely to be incorrect (Drukier 1996). Nevertheless, a more realistic treatment would make almost no difference to our results, as the mass fraction in neutron stars rarely exceeds 1 percent for our assumed IMF (Fig.1d).

The last issue to be addressed concerns the scaling from time in N-body units to astrophysical units; as we want to include the effects of disk shocking and stellar evolution, an appropriate time scaling is necessary not only for a correct application of N-body results to real clusters but also for a proper determination of the times when the mass of stars must be removed due to stellar evolution and the change in the velocities of stars due to disk shocking have to be made. An extensive investigation of this issue has been carried out by Aarseth & Heggie (1997a) (see also Fukushige & Heggie 1995) who have shown that, depending on the time scale of the physical process (stellar evolution or relaxation) determining the evolution of the cluster, the scaling must ensure that the ratio of "real" time to N-body time must be equal to the ratio of "real" to N-body crossing or relaxation time.

In fact, as discussed in Aarseth & Heggie (1997a), if the cluster lifetime is shorter than the time scale in which relaxation effects become important (e.g. because of strong mass loss due to stellar evolution causing the cluster to disrupt) the proper factor to scale N-body time to real time is given by the ratio of the crossing time of N-body system to that of the real system. On the other hand if the cluster survives for a time long enough to be affected by relaxation the proper conversion factor is provided by the ratio of relaxation times of N-body and real system thus ensuring that the number of relaxation times elapsed is the same in the N-body system and in the real cluster. Possibly a variable time scaling, taking into account the transition from a phase dominated by stellar evolution effects to one dominated by relaxation, might be the best choice (see Aarseth & Heggie 1997a for a detailed discussion of this point).

Since all the systems considered in our work do not disrupt quickly due to the effects of stellar evolution but survive

for a lapse of time during which relaxation effects become important, we have scaled time by the ratio of relaxation times (half-mass relaxation times have been used) of N-body to real system.

3 RESULTS: TWO-BODY RELAXATION AND STELLAR EVOLUTION

3.1 Global mass function

A set of simulations not including disk shocking have been run to establish to what extent differential escape due to two-body relaxation (and mass loss due to stellar evolution) can alter the mass function of a globular cluster. Since the evaporation rate due to two-body relaxation is larger for low-mass stars than it is for the high mass ones (see e.g. Spitzer 1987, Giersz & Heggie 1997 for some recent N-body simulations where this is clearly shown) a flattening of the IMF as dynamical evolution of a cluster proceeds is expected. This process could also be responsible for the observed correlation between the slope of the mass function and the galactocentric distance; in fact, as the evaporation rate is inversely proportional to the relaxation time, the largest changes in the IMF, for a fixed value of the cluster mass, are to take place closer to the galactic center where the size of clusters are smaller and the relaxation time shorter.

Table 1 summarizes the initial conditions and the main results for the set of runs done. The parameter F_{cw} is defined as

$$F_{cw} \equiv \frac{M_i}{M_\odot}\frac{R_g}{\mathrm{Kpc}}\frac{1}{\ln(N)}\frac{220\mathrm{km\ s}^{-1}}{v_c} \tag{8}$$

where M_i is the initial mass of the cluster, N the total initial number of stars, R_g the distance from the galactic center and v_c the circular velocity around the Galaxy. This parameter, introduced by Chernoff & Weinberg (1990), is proportional to the relaxation time and thus clusters having the same value of F_{cw} form a family of models evolving in the same way provided that relaxation dominates (obviously this is true for clusters all with the same initial concentration and IMF). Both the initial concentration and the slope of the IMF have been varied in order to investigate the dependence of the results on these quantities. The slope of the mass function, at $t = 15$ Gyr, reported in Table 1 is that measured for main sequence stars with $0.1 < m/m_\odot < 0.5$.

It is evident that evaporation through the tidal boundary due to two-body relaxation gives rise to a significant trend between the slope of the MF and the distance from the galactic center. As the results of runs starting with $W_0 = 5$ show, the trend established does not depend significantly on the initial concentration. On the other hand, the slope of the IMF seems to have a more important effect on the formation of this correlation, and more in general on the extent the IMF evolves, as shown by the results of the runs with $\alpha_i = 3.5$. In this case the differences between the initial and the final value of α are much smaller than for runs starting with a flatter MF and the trend between α and the galactocentric distance is much weaker. As is evident from the data in the table, there is a clear relationship between the amount of mass which has escaped from the cluster and the variation of its mass function (we will go through this point in greater detail later in the paper) and the smaller changes in α for these runs simply reflect the smaller mass loss rate for these systems.

We now focus our attention on the runs with $\alpha_i = 2.5, W_0 = 7, M_i = 6.15 \times 10^4 M_\odot$. Fig.1 shows the time evolution of some global quantities for this set of runs. Panel (c), where the time evolution of the total number of particles in the first and the fifth bin (corresponding to a range of masses $0.1 < m/m_\odot < 0.12$ and $0.25 < m/m_\odot < 0.31$ respectively) of the mass function for the run at $R_g = 4$Kpc and for that at $R_g = 16$ Kpc has been plotted, clearly shows the preferential escape of low-mass stars which is responsible for the flattening of the IMF. As shown in panel (f) the evolution of α is quicker for clusters at smaller galactocentric distances and this gives rise to the correlation between α and R_g. Finally it is interesting to note from panel (e) that the fraction of the total mass of a system in white dwarfs increases as the total mass of the cluster decreases (see sect.3.2 for further discussion on all the issues concerning white dwarfs).

In fig.2 the MF at $t = 0, 7, 10, 15$ Gyr for main sequence stars for the run at $R_g = 4$ Kpc is plotted to show the progressive flattening of the MF.

The data available and discussed above refer to a very limited set of initial conditions; nevertheless, besides being important for the indications they have provided, the results of these runs can be used to derive some general analytical expressions for the main quantities of interest for our work which will allow the results to be extended to a larger set of initial conditions. From the data of these runs it is possible to derive expressions providing the total mass of a cluster, the slope of the MF and the fraction of white dwarfs at any time t, for any value of the initial mass and any value of the galactocentric distance within reasonable limits we will see below. Let's start by investigating the behaviour of the total mass of the cluster. The total mass of a cluster decreases as a result of the mass loss due to stellar evolution and two-body relaxation. For a given initial value of α (and fixed values of the lower, m_{low}, and upper, m_{up}, limits of the MF) the fractional mass loss due to stellar evolution is the same for all clusters no matter what their initial mass is or what their galactocentric distance is. For the stellar evolution model adopted in this work this can be explicitly written as a function of the stellar mass at turn-off, $\tilde{m}$.

Having defined the following functions

$$F_1(\tilde{m}) = \frac{m_{up}^{2-\alpha} - \tilde{m}^{2-\alpha}}{m_{up}^{2-\alpha} - m_{low}^{2-\alpha}} - 1.4\left(\frac{2-\alpha}{1-\alpha}\right)\left(\frac{m_{up}^{1-\alpha} - \tilde{m}^{1-\alpha}}{m_{up}^{2-\alpha} - m_{low}^{2-\alpha}}\right) \quad \text{for } 8 < \tilde{m}/m_\odot < m_{up}$$

$$F_2(\tilde{m}) = \frac{8^{2-\alpha} - \tilde{m}^{2-\alpha}}{m_{up}^{2-\alpha} - m_{low}^{2-\alpha}} \quad \text{for } 4.7 < \tilde{m}/m_\odot < 8 \tag{9}$$

$$F_3(\tilde{m}) = 0.78\left(\frac{4.7^{2-\alpha} - \tilde{m}^{2-\alpha}}{m_{up}^{2-\alpha} - m_{low}^{2-\alpha}}\right) - 0.36\left(\frac{2-\alpha}{1-\alpha}\right)\left(\frac{4.7^{1-\alpha} - \tilde{m}^{1-\alpha}}{m_{up}^{2-\alpha} - m_{low}^{2-\alpha}}\right) \quad \text{for } m_{low} < \tilde{m}/m_\odot < 4.7$$

we can write the fractional mass loss due to stellar evolution as

$$\frac{\Delta M_{st.ev.}}{M_i} = \begin{cases} F_1(\tilde{m}) & \text{if } 8 \le \tilde{m}/m_\odot < m_{up} \\ F_1(8) + F_2(\tilde{m}) & \text{if } 4.7 \le \tilde{m}/m_\odot < 8 \\ F_1(8) + F_2(4.7) + F_3(\tilde{m}) & \text{if } m_{low} \le \tilde{m}/m_\odot < 4.7 \end{cases} \tag{10}$$

To calculate the total mass loss due to stellar evolution at any time t it is necessary to know the turn-off mass at that time; this is derived by interpolating the data provided in Table 1B of Chernoff & Weinberg (1990). In fig.3a the time evolution of the total mass is presented. We plot separately that due to mass loss associated with stellar evolution and that due to other processes, i.e. mainly two-body relaxation and the effect of the tide.

The latter shows clearly its dependence on the initial conditions of the mass loss due to the latter process and its linear dependence on time. We point out that while the amount of mass loss due to stellar evolution obtained by eq. (10) does not consider the possibility that some stars might escape from the cluster before losing their mass, the curves obtained from N-body data include only mass loss from stars inside the tidal boundary of the cluster; for the IMF chosen in our simulations the great majority of escaping stars have masses smaller than those evolving before 20 Gyr and thus the theoretical estimate and the data from simulations are almost coincident.

In fig.3b we show that, scaling the time by the parameter F_{cw}, all the curves representing the time evolution of the total mass (considering only the mass loss by two-body relaxation) at different galactocentric distances coincide. Thus we can write

$$\frac{M(t)}{M_i} = 1 - \frac{\Delta M_{st.ev.}}{M_i} - \frac{\beta}{F_{cw}}t \tag{11}$$

where β is a constant that can be determined by a linear fit of the curves shown in fig.3b and is found to be $\beta \simeq 0.828$ (calculated as the mean value of the slopes of the curves shown in figure 3b where time is measured in Myr). Eq.(11) allows us to calculate the mass of a cluster at any time t for a cluster with initial mass M_i and located at a distance from the galactic center R_g; only a slight difference in the value of β has been found for systems starting with $W_0 = 5$, which in this case is $\beta \simeq 0.790$. Fig.4 shows a 3-d plot of $M(15Gyr)/M_i$ as a function of M_i and R_g and a contour plot of this function. The more massive clusters and those located at larger distances from the galactic center are those which preserve a larger fraction of their initial mass as two-body relaxation is less and less efficient and the only mass loss is due to stellar evolution.

Though it is not the purpose of this paper to consider the lifetimes of the globular clusters, it interesting in passing to compare our result with some others which have been used in discussions of the evolution of the Galactic globular cluster system. It is shown in Aarseth & Heggie (1997a) that the lifetime obtained by the methods we use are in satisfactory agreement with those determined by Chernoff & Weinberg (1990) using the Fokker-Planck method. Aguilar et al. (1988) used two different expressions for the lifetime (due to escape by two-body relaxation) of a tidally bound cluster, but only for clusters with stars of equal mass. We find that the lifetimes for a typical model given by their formulae exceed our by a factor of about three or four. Chernoff, Kochanek & Shapiro (1986) also neglected stellar evolution but did include several additional mechanisms such as disk shocking. Even so their lifetimes exceed ours (which in this section do *not* include disk shocking) by a factor of two in typical cases. Typical lifetimes to evaporation (by two-body effects alone, but with stars of equal mass) given by Gnedin & Ostriker (1997) exceed ours by about 40 percent.

In order to obtain an analytical expression for the slope of the mass function it is necessary to estimate the evaporation rate for stars with different masses. If the mass function is $dN \propto m^{-\alpha}dm$ we can write for any values of the mass of stars m_1 and m_2

$$\alpha = -\frac{\ln(dN/dm)_1 - \ln(dN/dm)_2}{\ln m_1 - \ln m_2}. \tag{12}$$

We estimate $(dN/dm)_{1,2}$

$$\left(\frac{dN}{dm}\right)_{1,2} = \frac{N_{1,2}(t)}{\Delta m_{1,2}} \tag{13}$$

where $N_{1,2}(t)$ is the total number of stars with mass between $m_{1,2}$ and $m_{1,2} + \Delta m_{1,2}$ at time t. It is found from our results that the time evolution of total number of particles with a given mass is approximately linear and the slope is inversely proportional to the parameter F_{cw}

$$N_1 = N_1(0)\left(1 - \frac{\xi_1 t}{F_{cw}}\right) \tag{14}$$

It follows that the slope of the mass function at time t can be written as

$$\alpha(t) = \alpha(0) - \frac{\left[\ln\left(1 - \frac{\xi_1 t}{F_{cw}}\right) - \ln\left(1 - \frac{\xi_2 t}{F_{cw}}\right)\right]}{\ln m_1 - \ln m_2} \tag{15}$$

We have chosen $m_1 = 0.1 m_\odot$ and $m_2 = 0.5 m_\odot$ (this being the range where our values of α are calculated). ξ_1 has been estimated by a linear fit of the curve $N_1(t)$ for the run with $R_g = 16$ Kpc (for 5 $Gyr < t <$ 10 Gyr where it has a definite linear behaviour). By fitting the values of $\alpha(15 Gyr)$ from our runs at different R_g with the function (15) we have determined ξ_2. Thus we get the following estimate for the slope of the mass function at time t for a cluster with initial mass M_i orbiting at a distance R_g from the galactic center

$$\begin{aligned}\alpha(t, R_g, M_i) = \quad & 2.5 + 0.62\left[\ln\left(1 - 1.1506\left(\frac{t}{Myr}\right)\left(\frac{Kpc}{R_g}\right)\left(\frac{M_\odot}{M_i}\right)\ln(M_i/0.28)\right)\right. \\ & \left. - \ln\left(1 - 0.2715\left(\frac{t}{Myr}\right)\left(\frac{Kpc}{R_g}\right)\left(\frac{M_\odot}{M_i}\right)\ln(M_i/0.28)\right)\right]\end{aligned} \tag{16}$$

where we have taken $v_c = 220 \mathrm{km\ s^{-1}}$ and $0.28 m_\odot$ is the initial mean stellar mass for the IMF adopted in our work. By eq.(11) it is also possible to calculate α at any given time t, for a cluster located at R_g and whose mass at time t is $M(t)$. Fig.5 shows the curves of α(15Gyr) as a function of the galactocentric distance for clusters having the same initial mass. Eq.(16) is valid as long as the number of particles is a linear function of time; it is possible to see from fig. 1a that towards the end of the cluster lifetime, the behaviour of $N(t)$ deviates from the linear scaling with time and slows significantly. The linear regime ends approximately at $t \sim 8.5 \times 10^{-4} F_{cw}$ Gyr (or equivalently when $M_f/M_i \sim 0.11$); for values of t larger than this, eq.(16) will provide a slope of the MF smaller (i.e. a flatter MF) than the real one.

Thus, in the plane $\alpha - R_g$, stellar mass loss and evaporation due to two-body relaxation cause points , initially on the line $\alpha(R_g) = 2.5$, to spread into the strip shown in fig.5.

While the curves on this diagram are qualitatively consistent with the correlation between α and R_g observed for Galactic globular clusters (see below), much caution would be needed in the use of these results in any *detailed* interpretation of observations. In the first place the observational data themselves are subject to considerable uncertainty from a variety of sources, including the distinction between global and local luminosity functions, the questionable reliability of ground-based data, and our poor knowledge of the mass-luminosity relationship for low-mass stars. Next, there are limitations in our modelling, including the use of circular orbits and a single initial mass function, and measurement of the mass function over a single range in mass. Also, we have found that the time scale on which the MF evolves is heavily determined by the initial total mass, which is unknown for observed clusters.

One assumption of our models we have been able to check is the influence of primordial binaries, by comparison with models discussed by Aarseth & Heggie (1997b in preparation). Inclusion of 10 percent hard binaries by number appears to decrease α by an amount of order 0.05 (i.e. the mass function is flattened); this is small compared to the evolutionary changes and fluctuations in the data (cf. Fig.6), and may not be significant.

Despite the caveats it is still interesting to compare our results with a representative sample of mass function slopes from the literature. For example Capaccioli et al. (1993) have summarised ground-based data for 17 clusters and they find a dependence of α on the current value of R_g which is quite similar (qualitatively and quantitatively) to that of Fig.5 for relatively low initial masses ($\lesssim 10^5 M_\odot$). To go further it would be necessary to give attention to most caveats stated above. For example, Fig.13 (below) shows that disk shocking increases the evolution of α beyond that indicated in Fig.5, while our values of α are measured for stars of lower mass than is the case with the observational data. Furthermore, it might be more realistic to compare our simulations with observational data for the dependence of α on the estimated *perigalactic* distance of the clusters.

Incidentally it is often implied that the observed correlation is a signature of disk shocking. We have, however, shown that relaxation by itself can significantly affect the shape of the IMF in a manner qualitatively consistent with observation.

3.2 Local mass function

We turn now our attention to the differences between the global/initial mass function and the local mass function measured at various distances from the cluster center. Since in some cases observational data are taken for different clusters at different distances from the cluster center it is important to understand how large the difference between a local MF and the global one can be and where, inside the cluster, this difference is larger, as well as to establish whether and where the PDMF keeps memory of the IMF.

We have calculated the slope of the MF in three shells: the innermost shell extends from the center to r_{30}, where r_{30} is the radius containing the innermost 30% of the total number of stars; the intermediate shell extends from r_{30} to r_{60} and the outermost shell extends from r_{60} to r_{100} (both 3-d and 2-d (projected distance) shells have been considered). The limits of the three shells compared with the half-mass radius of the cluster, r_h, are approximately $(0-0.8r_h), (0.8-1.6r_h), (1.6-4r_h)$. We focus our discussion on the results for the run at $R_g=4$ Kpc and for that at $R_g=16$ Kpc. The former undergoes a strong mass loss and evolution of the global value of α while, in the latter, mass loss due to two-body relaxation is negligible and α does not change significantly.

If only mass segregation takes place and no star escapes from the cluster due to relaxation, the mass function of the innermost shell becomes flatter during the evolution while the MF of the outermost one becomes steeper. What happens when there is some mass loss depends on how strong this is and on how efficient it is in counteracting the trend given by mass segregation. In fact, while the MF of the inner shell will always tend to become flatter, the shape of the MF of the outermost shell depends on the relative efficiency of two processes acting in opposite directions: mass segregation tends to steepen the MF, evaporation tends to flatten it down. Figs. 6a-d show the time evolution of the MF in 2-d and 3-d shells for the runs at $R_g=4$ Kpc and $R_g=16$ Kpc. The above qualitative scenario is evident from figs. 6a-b, relative to the run at $R_g=4$ Kpc: the MF of the innermost shell immediately flattens, that of the intermediate shell initially preserves its initial slope but eventually flattens, and the MF of the outermost shell after an initial stage during which tends to undergo a slight steepening eventually flattens when mass loss effects dominate mass segregation.

At $R_g=16$ Kpc the only relevant effects are those due to mass segregation and, as shown in figs. 6c-d, the slope of the MF is flatter than the initial one in the inner shells and steeper than the initial MF in the halo. We note that in this case no significant mass loss occurs and the MF near the half-mass radius resembles quite well the IMF (Richer et al. 1991, by an analysis of multi-mass King models, arrived at the same conclusion), but we emphasize that the results for the run at $R_g=4$ Kpc, show this is not always the case, since, if a significant mass loss takes place, the PDMF at r_h has no relationship with the IMF after a few Gyr.

To provide a quantitative estimate of the difference between the initial/global MF and the local MF we have calculated the following quantities

$$\Delta\alpha_{glob}=\alpha_{shell}-\alpha_{glob}, \tag{17}$$

and

$$\Delta\alpha_i=\alpha_{shell}-\alpha_i. \tag{18}$$

A negative (positive) value of these quantities means that the local MF is flatter (steeper) than the global/initial MF. The time evolution of the above quantities for the 3-d shells (no qualitative difference is present in their behaviour for the 2-d shells) is shown in figs 7a-d. At $R_g=4$ Kpc a strong mass loss takes place which eventually makes the MF of all the shells flatter than the IMF. On the other hand when the local MFs are compared with the global MF, the effects of mass segregation are evident as the outermost shell MF and the innermost shell MF are respectively steeper and flatter than the global one. The intermediate shell MF quite well resembles the global one during the entire evolution. At $R_g=16$ Kpc the mass loss due to two-body relaxation is negligible and the global MF barely changes during the entire simulation. In this case mass segregation is the only process at work and the results obtained are in agreement with what is expected.

From the above results we can draw the following conclusions: 1) the MF in the outer shells of a cluster is always steeper than the global one but it can be much flatter than the IMF if strong mass loss occurred, thus changing it significantly; this means that observational data taken in the outer regions of a cluster may be of no help in getting any information about the IMF if the cluster has undergone a significant dynamical evolution; 2) the MF near the half-mass radius is the most similar to the global one and thus it can be significantly different from the MF in more external regions of the cluster, always in the sense that the external MF is steeper; much caution should be used in comparing observational data taken at different distances for different clusters and modelling of mass segregation effects (see e.g. King, Sosin & Cool 1995) when any comparison is to be done is necessary.Though it is not the purpose of this paper to investigate mass segregation as such, it is of interest to see how well its effect on the local mass function slope can be modelled with a multi-mass anisotropic King model. For the sake of illustration we took a model with initial mass $1.49\times10^5 M_\odot$ and IMF index $\alpha=2.5$ at galactocentric radius $R_g=4.4$ kpc, and examined its structure at 20 Gyr. This is a post-collapse model which has lost a little over half its mass and about 20 percent of its remaining mass is in the form of white dwarfs (see section 3.3). The stars were binned uniformly in $\log M$ in

the range $0.1M_\odot < m < M_\odot$ and in Lagrangian radii corresponding to 10 uniformly spaced bins by total number. The white dwarfs were added to the bin of stars with average mass about $0.45M_\odot$. Next a King model was selected to fit the central parameters of all species and, by variation of the remaining free parameters, the density profile of the stars of average mass about $0.56M_\odot$. Finally the spatial profile of α in the King model, computed as in the N-body models, was compared with the N-body result. It was found that the value of α in the King model was slightly but sistematically smaller (by an average of about 0.4) than in the N-body model, except in the inner 10 percent, where the models were forced to agree. Undoubtedly a post-collapse model is a strenuous test of model fitting, and such a significant discrepancy would not be expected in less evolved models.

Any difference in the MFs of two clusters observed at different distances from the center does not necessarily imply their global MF are different and in any case their difference is likely not to signify the real difference between the global MFs.

3.3 White dwarfs

The code we have used for our investigation includes the effects of stellar evolution according to the same model used in Chernoff & Weinberg (1990). Besides studying the effects of this process on the dynamical evolution of a cluster it is thus possible to address the issue of the presence of degenerate remnants in the cluster, white dwarfs and neutron stars. As for the neutron stars these are found to be a very small fraction of the total mass after 15 Gyr and no systematic investigation has been possible due to the small numbers involved. It has been possible to do much more for the white dwarfs. In table 1 the ratio of the total mass in white dwarfs to the total mass at $t = 15$ Gyr for all the runs done is shown. The first point coming out from the data is that the smaller the final value of the total mass, the larger the fraction of the mass in white dwarfs. The fraction of mass in white dwarfs results from two opposite processes: the production of white dwarfs from stars with initial mass less than 4.7 $m_\odot$ evolving from the main sequence and the loss by evaporation through the tidal boundary of the white dwarfs which have already formed or, possibly, of their main sequence progenitors. For a power-law IMF with lower limit, m_{low}, and upper limit m_{up}, the ratio of the total mass in white dwarfs, M_{wd}, produced at a time t, when the turn-off mass is $\tilde{m}$, to the initial mass M_i is given by

$$\left(\frac{M_{wd}}{M_i}\right)_{prod} = \begin{cases} 0 & \text{if } \tilde{m}/m_\odot > 4.7 \\ \frac{2-\alpha}{m_{up}^{2-\alpha}-m_{low}^{2-\alpha}}\left[\frac{0.36}{1-\alpha}(4.7^{1-\alpha}-\tilde{m}^{1-\alpha})+\frac{0.22}{2-\alpha}(4.7^{2-\alpha}-\tilde{m}^{2-\alpha})\right] & \text{if } \tilde{m}/m_\odot < 4.7. \end{cases} \tag{19}$$

The above expression would provide the total mass of white dwarfs if no loss of stars took place. Actually a certain fraction of the white dwarfs produced escapes and this expression provides only an upper limit for M_{wd}. The real value of M_{wd}/M_i can be written as the product of the eq.(19) by a function of time taking into account the reduction of the expected mass in white dwarfs due to the loss of stars through the tidal boundary

$$\left(\frac{M_{wd}}{M_i}\right)_{real} = \left(\frac{M_{wd}}{M_i}\right)_{prod} \times F(t) \tag{20}$$

The function $F(t)$ has to be determined by the results of N-body simulations. In fig. 8a we show the time evolution of M_{wd}/M_i for the runs starting with $W_0 = 7$, $\alpha_i = 2.5$ and $R_g = 4, 5, 8, 16$ Kpc. Also shown in the figure is $\left(\frac{M_{wd}}{M_i}\right)_{prod}$ which, as expected, always lies above the curves corresponding to the data from N-body simulations. The function $F(t)$ obtained from the ratio of M_{wd}/M_i from N-body data to $(M_{wd}/M_i)_{prod}$ (eq.19) is shown for the same runs in fig. 8b. In fig. 8c the same function, this time for all the runs (both $W_0 = 5$ and $W_0 = 7$), versus the time scaled by the parameter F_{cw} is shown. As expected some spread is still present among curves corresponding to different initial conditions; in fact even though the effect of two-body relaxation in causing stars to evaporate from a cluster is the same for the same value of the scaled time, the properties of the population of white dwarfs (their mass distribution essentially) is different and a difference in the fraction of escaped white dwarfs is thus expected. Nevertheless this difference is not very large and we can approximately write $F(t)$ as a unique function of the scaled time, t/F_{cw}. In order to obtain an analytic expression for this function, we have done a polynomial fit of the data obtained from the two runs at $R_g = 4$ Kpc starting with $W_0 = 7$ and $W_0 = 5$ (fig.8d)

$$F(t, R_g, M_i) = F(t/F_{cw}) = 1 - 0.794\frac{t}{F_{cw}} + 7.12 \times 10^{-5}\left(\frac{t}{F_{cw}}\right)^2 - 3.82 \times 10^{-9}\left(\frac{t}{F_{cw}}\right)^3 \tag{21}$$

which provides a good approximation for $t < 9 \times 10^{-4} F_{cw}$ Gyr (or equivalently for $M_{fin}/M_i > 0.07$). By the above equations we can predict the fraction of the total (initial or at any time t) mass in white dwarfs at any time t for clusters at a galactocentric distance R_g (Kpc) with an initial mass M_i ($M_\odot$) or equivalently for clusters having a family parameter $F_{cw} = M_i R_g/\ln(M_i/0.28)$ (0.28 being the mean value of the mass for the IMF we are considering and for which the analytic expression of $F(t, R_g, M_i)$ is valid).

In fig. 9 we show the plot of $M_{wd}/M(15Gyr)$ versus F_{cw}: $M_{wd}/M(15Gyr)$ is a decreasing function of F_{cw} and this means that the fraction of the total mass in white dwarfs is larger for clusters undergoing a strong dynamical evolution and losing a

large fraction of their initial mass; the smaller the ratio of the final to the initial total mass is, the larger the fraction of the final mass in white dwarfs is. Fig.10 shows the plot of $M_{wd}/M(15Gyr)$ versus the logarithm of the total mass of the cluster at $t = 15$ Gyr for different values of R_g. Not very much is currently known about the fraction of white dwarfs in globular cluster from observations; the only estimates are supplied by authors using observed light (and velocity dispersion) profiles to model the structure and the stellar content of individual globular clusters usually by multi-mass King models (see e.g. Meylan 1987 and references therein).

Following this method, the fraction of white dwarfs is estimated assuming that the current value of the slope of the MF is equal to that of the IMF and, consistently, that the only mass loss that occurred during the cluster lifetime is due to stellar evolution (hereafter we will refer to this estimate as the 'observational' estimate). It is clear that if mass loss due to relaxation takes place and, as a consequence of this the IMF is different from the present one, this procedure will not provide a correct estimate of the content of white dwarfs. Assuming that the slope of the IMF is equal to 2.5, we can use the results of our simulations to provide a quantitative estimate of the error incurred. Fig.11a shows the contour plot of $M_{wd}/M(t)$ in the plane $t - \alpha(t)$ providing the value of $M_{wd}/M(t)$ for any cluster once the slope of its mass function and the time this value of the slope is reached are known (assuming the initial value of α is equal to 2.5); dashed lines show the evolution of α for clusters with different values of F_{cw} obtained from eq. (16). Fig.11b shows an analogous plot but in this case the values of $M_{wd}/M(t)$ are the 'observational' estimates. Finally fig.11c shows the contour plot of the ratio of the two above estimates of $M_{wd}/M(t)$ (the estimate from N-body data to the observational one) and it provides the correction to be made to the ' observational' estimate; the latter overestimates the content of white dwarfs but the error made for the fraction of white dwarfs at $t = 15$ Gyr is never too large, as the correction to be made is never smaller than about 0.65 at $t = 15$ Gyr. Figs. 12a-c show plots analogous to those of figs. 11a-c but in the plane $\log M(15\mathrm{Gyr})$-R_g.

4 RESULTS:DISK SHOCKING

In this section we will show the results of a set of simulations including the effects of disk shocking. The main goal is that of investigating to what extent this process can alter the results described in the previous section in which only stellar evolution and relaxation were considered.

We begin by making some preliminary qualitative considerations about the expected changes due to disk shocking in the three quantities (total mass, white dwarf content and MF slope) we have focussed our attention on until now.

As for the total mass, it is obvious that disk shocking will cause an additional mass loss and the total mass of a cluster at any time t will be (depending on the strength of disk shocking) less than or equal to the corresponding value for a cluster starting with the same initial conditions but not undergoing disk shocking. It is not so obvious what to expect for the content of white dwarfs; no simple qualitative argument can predict if the same correlation between the fraction of total mass in white dwarfs and the ratio of total to initial mass, shown to hold in the previous section, still holds in this case. In fact, it is not possible to know, *a priori*, if the mass lost by disk shocking will contain the same fraction of white dwarfs it would contain if this additional mass loss were due to two-body relaxation. Analogous information is required to predict the effects of disk shocking on the evolution of the MF. As for this latter issue one difference between the mass loss due to disk shocking and that due to two-body relaxation is that, contrary to what happens for mass loss due to two-body relaxation, disk shocking does not produce any differential escape of stars with different mass unless the masses are segregated by some other mechanism; the change in the velocity of a star due to disk shocking, for a cluster at a given galactocentric distance, depends only on the distance from the cluster center and not on the mass of the star. This means that only with the joint effect of mass segregation, driving low mass stars into the halo and high-mass stars into the core, can the mass loss due to disk shocking alter the slope of the mass function. The extent to which disk shocking can alter the mass function thus depends not only on the mass loss but also on mass segregation.

Initial conditions and the main results for the runs including disk shocking are shown in table 2. Besides running simulations with the same initial conditions adopted for runs without disk shocking, we have investigated a set of initial conditions having the same galactocentric distance but different values of the initial mass (and thus different values of F_{cw}) and a set of initial conditions all having the same value of F_{cw} but different galactocentric distances. The former set have been investigated in order to determine the differences in the effects of a sequence of interactions with a disk having the same strength (fixed R_g) on clusters having different values of F_{cw}, while the latter have been done to study the effects of disk shocking with a varying strength on clusters all having the same initial value of F_{cw}. The results of these runs, besides providing useful indications on the effects of disk shocking on the stellar content of globular clusters, should make possible the derivation of more general expressions for the total mass, the slope of the MF and the fraction of the total mass in white dwarfs (eqs.(11,16,20)).

In fig.13 we have plotted the slope of the MF after 15 Gyr as a function of the galactocentric distance, showing to what extent disk shocking has changed the final result expected for runs starting with the same initial conditions but not undergoing disk shockings.

Besides the same quantities already shown in table 1 for the runs without disk shocking, the fraction of the initial mass

lost by disk shocking $\Delta M_{ds}/M_i$ and the additional change in the slope of the MF due to disk shocking have been included in table 2. Both of these quantities have been calculated as the difference between the values obtained from the simulations with disk shocking and the results expected for the same initial conditions without the effects of disk shockings, the latter being calculated by eqs.(11,16). In figs. 14a-b the evolution of the total mass and of the slope of the MF for the runs not including disk shocking is compared with that obtained from runs with the same initial conditions and including the effects of disk shocking. In agreement with what is expected, the evolution of both the total mass and the MF is faster for systems undergoing disk shocking (except for the system at $R_g = 16$ Kpc where the effects of disk shocking are negligible and the differences are due to statistical fluctuations).

These plots provide generic information on the effects of disk shocking, but the most important information to answer the questions raised above concerning the fraction of white dwarfs contained in the mass lost by disk shocking and the effect of this process on the evolution of the slope of the mass function comes from the plots shown in figs. 15-16.

In these figures the fraction of the total mass at $t = 15$ Gyr in white dwarfs and the difference between the initial slope of the MF and that at $t = 15$ Gyr are plotted against the ratio of the total mass at $t = 15$ Gyr to the initial one; the values predicted from the analytical expression derived in the previous section for the runs without disk shocking are also shown. Both the change in the slope of the MF and the content of white dwarfs depend only on the fraction of mass lost during the evolution no matter whether relaxation is the only process causing the evaporation of stars or disk shocking is also responsible for a part of the escaping stars. This means that the content of the fraction of mass lost by disk shocking is similar to that lost by two-body relaxation. We note that, even though the values of the final mass we have plotted in fig.16 are determined both by mass loss due stellar evolution and relaxation/disk shocking/tidal stripping, obviously the relevant quantity in determining the variation in the slope of the IMF (for main sequence stars) is only the escape of stars due to relaxation/disk shocking/tidal stripping. Since the data plotted refer to systems all with the same IMF and thus all losing by stellar evolution the same fraction of their initial mass,the difference between the real final mass and the final mass calculated considering only the escape of stars by relaxation/disk shocking is equal to a constant (~ 0.18 for the IMF adopted in our work; in fact $\alpha_i - \alpha(15)$ tends to 0 for $M_f/M_i \simeq 0.82$ that is when the only mass loss is due to stellar evolution). Should data from systems losing a different fraction of their initial mass by stellar evolution be considered for this plot, this correction should be properly taken into account.

The same remark applies to fig.15; in this case also the dependence on the IMF of the total mass of white dwarfs produced should be considered.

If, analogously to what was done for the runs without disk shocking, we could get an analytical expression for the time evolution of the mass, we might then use the relationship between this quantity and the fraction of white dwarfs and the slope of the MF to obtain these quantities at any time t and for a quite general set of initial conditions.

Fig. 17 shows the time evolution of the total mass for four different runs including disk shocking, two for initial conditions with the same value of F_{cw} and two for initial conditions having the same galactocentric distances. The mass lost by stellar evolution has been added so that the plotted lines show only the mass lost by disk shocking and two-body relaxation. Similarly to what happens when disk shocking is not included, the mass is a linear function of time. This and the results coming from figs. 15-16 suggest that it is possible for any initial condition to define an *equivalent family parameter*, F_{cw}^{eq} having the following meaning: the evolution of a cluster with a family parameter F_{cw} whose evolution is driven by both two-body relaxation and disk shocking is equivalent to that of cluster whose evolution is driven by two-body relaxation only but whose family parameter is F_{cw}^{eq}, where $F_{cw}^{eq} \leq F_{cw}$ always. Of course F_{cw}^{eq} depends on F_{cw} and on R_g and the main goal is now that of finding out this dependence by which we will be able to calculate analytically any quantity we are interested in once the initial conditions are specified, exactly as we have done in the previous section.

In the previous section we have shown that the mass loss is a linear function of time and that the mass loss rate is inversely proportional to the family parameter F_{cw}; in order to get an analytic expression for F_{cw}^{eq} we have calculated from the results of our N-body simulations an empirical analytical expression for the mass loss rate as a function of F_{cw} and R_g and derived from this F_{cw}^{eq}. Analogously to what was done for the runs without disk shocking, we can write

$$\frac{M(t)}{M_i} = 1 - \frac{\Delta M_{st.ev.}}{M_i} - \lambda t; \tag{22}$$

as shown in the previous section, when two-body relaxation is the only process considered, λ depends only on F_{cw} ($\lambda = \beta/F_{cw}$, see eq.(11)); if the effects of disk shocking also are taken into account λ depends both on F_{cw} and on R_g. From our data we find

$$\log\lambda = 0.6931 - 1.46\log R_g - 1.134\log F_{cw} + 0.2916\log F_{cw}\log R_g. \tag{23}$$

The above expression is completely empirical and it has been derived from data spanning a limited range of values of R_g ($1.1 < R_g < 16$) and $F_{cw}(2\times10^4 < F_{cw} < 1.13\times10^5)$ but it nevertheless provides useful qualitative and quantitative information on the evolution of clusters including the effects of disk shocking. The plot of λ obtained from N-body data versus the value calculated from eq.(23), fig. 18, shows that eq.(23) approximates well the dependence of λ on F_{cw} and R_g.

As explained above, once λ is known, we can easily calculate F_{cw}^{eq}; fig.19a shows the ratio of the total mass at $t = 15$Gyr to the initial mass versus F_{cw} for all the runs done, both with and without disk shocking, with the solid line showing the values predicted from eq.(11). As expected the real value of F_{cw} does not provide a good indication of the mass loss for the runs with disk shocking; if F_{cw} is replaced by F_{cw}^{eq} (of course no difference exists between these two quantities for runs without disk shocking) all the data are located, with a good approximation, along the curve predicted by eq.(11) (fig.19b).

In fig. 20 families of models having given values of F_{cw} and F_{cw}^{eq} are shown; the qualitative behaviour agrees with what one would expect: two clusters located at the same galactocentric distance, one undergoing disk shocking and one not, evolve in the same way if the initial mass of the former is larger than that of the latter, while if they have the same initial mass, they evolve in the same way if the former is located at a galactocentric distance larger than the latter.

Analogous information is contained in fig. 21 where curves of equal-mass at $t = 15$ Gyr are shown for clusters evolving with and without disk shocking in the plane $\log M_i - R_g$.

We can now calculate analytically α and the content of white dwarfs at any time t and for any initial condition (within the limits mentioned in this and in the previous section and for the particular choice of IMF adopted in our work) taking into account also the effects of disk shocking.

Fig. 22 shows the changes due to disk shocking in the curves of $\alpha(15Gyr)$ versus R_g for different values of the initial mass. As for the formation of a correlation between the slope of the mass function and the galactocentric distance, as could be seen already from fig. 13 , disk shocking has the effect of increasing the trend established by two-body relaxation.

5 DEPENDENCE OF THE RESULTS ON N

By the simulations described in the previous sections, starting with $N = 4096$ particles, we are trying to model the evolution of stellar systems typically having $N \simeq 10^6$ stars; the time scaling adopted to convert time in N-body units to astrophysical units should allow a proper use of the N-body data to investigate the evolution of real clusters. Nevertheless, as shown also in Aarseth & Heggie (1997a), a slight dependence of the results on N still exists. In order to give a quantitative estimate of the extent of the N-dependence we have done seven runs starting with the same initial conditions ($W_0 = 5, R_g = 4$ Kpc, $M_i = 6.15\times10^4 M_\odot$) but with a different initial number of particles (four runs with $N = 4096$, two runs with $N = 8192$ and one run with $N = 16384$ so as to have quantities all with the same statistical significance for all the values of N investigated). In table 3 we summarize the relevant information on these runs.

In agreement with the results of Aarseth & Heggie (1997a), we find that the larger the number of particles is, the faster the evolution of the system is. Part of the explanation of this is likely to reside in the differences in the structure of clusters with different N at the end of the initial phase dominated by mass loss due to stellar evolution. In fact, as explained in larger detail in Aarseth & Heggie (1997a), scaling time from N-body units to astrophysical units by the ratio of N-body to real relaxation time implies that the smaller the number of stars is, the smaller the ratio of time scale of mass loss due stellar evolution to the crossing time scale is. This is quite important since it is well known (see e.g. Hills 1980, Lada, Marculis & Dearborn 1984, Fukushige & Heggie 1995, Aarseth & Heggie 1997a) that the rate at which mass loss occurs plays an important role in determining the evolution of a stellar system, spanning from an expansion of the entire cluster proportional to $1/M$ without the escape of any star in the case of slow mass loss to the complete disruption of the cluster in the case of rapid mass loss exceeding 1/2 of the entire initial mass of the cluster; this difference is likely to produce a difference in the final structure of clusters losing mass by stellar evolution in the impulsive or adiabatic regime. The subsequent differences in the mass loss rate are likely to be due, at least partially, to this difference even though further investigation on this point is needed. Some simulations with $N = 4096$ and $N = 8192$ not including stellar evolution have been carried out to test to what extent the above effect was actually able to explain the observed differences. The trend for system with larger values of N to evolve faster has been found to be still present, even though to a smaller extent. This means that part of the differences observed are unlikely to be due to the chosen scaling and their origin must be due to a real difference in the evolution of systems with different N not simply scaling with the relaxation time. We could not find a convincing explanation for this result but possibly the dependence on N of the depth of the potential well and the consequent dependence of the fraction of stars ejected from the core reaching the outer regions (see e.g. Giersz & Heggie 1994) might explain the observed differences.

Fig. 23, in which we have plotted the slope of $M(t/F_{cw})/M_i$, i.e. β, (excluding the mass loss due to stellar evolution) versus N, clearly shows the increase in the mass loss rate as N increases. A correction of approximately 20% seems to be necessary to the conversion from time in N-body units to time in astrophysical units adopted in the set of runs with $N = 4096$.

As shown in figs. 15 and 16, however, the runs for all values of N yield the same result for the way in which both the variation in the slope of the mass function and the content of white dwarfs at $t = 15$ Gyr depend on the fraction of initial mass left after 15 Gyr.

While further investigation on the N dependence of the results is still necessary, particularly for what concerns the origin of this dependence, in the light of this last result it is clear that the correction to be made just implies that our results from

simulations with $N = 4096$ at $t = 15$ Gyr would actually be more relevant for real clusters at $t = 12$ Gyr and that results from simulations at $t = 18$ Gyr would be those relevant for real clusters at $t = 15$ Gyr.

6 SUMMARY AND CONCLUSIONS

In this work we have carried out a large set of N-body simulations to investigate the dynamical evolution of globular clusters, focusing our attention on the effects of dynamical evolution on the stellar content of the systems; in particular we have investigated the evolution of the MF and of the fraction of the total mass in white dwarfs. The code used includes the effects of stellar evolution, two-body relaxation and disk shocking and takes the presence of the tidal field of the Galaxy into account. A set of different initial conditions for the structure of the cluster and for the galactocentric distance has been considered.

The dependence of the slope of the MF and of the fraction of white dwarfs on the initial conditions of the clusters has been explored and in particular we have determined to what extent the observed correlation between the slope of the MF and the galactocentric distance can result from the effects of dynamical evolution; we have tried to provide a quantitative estimate of the role played by relaxation and disk shocking. The dependence of the slope of the mass function on the location inside the cluster has been also investigated, our attention being focused on the differences between the local MF, the IMF and the global PDMF.

The main conclusions we can draw are:

(i) in agreement with what is expected, as a result of mass loss through the tidal boundary, both due to two-body relaxation and to disk shocking, the global mass function becomes flatter. For given initial parameters, mass loss is stronger for clusters closer to the galactic center, and, consequently, a trend between the slope of the MF and the galactocentric distance forms as evolution goes on. This trend is stronger for low-mass clusters, as these have shorter relaxation times and thus evolve more quickly than massive clusters. Both mass loss by two-body relaxation and disk shocking are important in causing the MF to flatten. By the results of N-body simulations we have derived an analytical expression for the slope of the mass function at any time t and for any initial value of the mass and of the galactocentric distance both with and without the effects of disk shocking.

The difference between the initial and the final (at $t = 15$ Gyr) slope of the MF has been shown to depend approximately only on the fraction of the initial mass lost and this dependence is the same no matter whether disk shocking is included or not.

(ii) The MF near the half-mass radius is the one which, during the entire evolution, is least affected by mass segregation and quite well resembles the present-day global mass function. The extent to which the MF observed near the half-mass radius can provide us with useful information on the IMF thus depends on the difference between the IMF and the PDMF. Possibly, when the the PDMF is different from the IMF, observations of the MF at radii larger than the half-mass radius can supply indications on the IMF, but it is important to note that, in cases of strong mass loss and evolution of the IMF, we have shown that, even the MF in the outer regions of the clusters eventually becomes flatter than the IMF whose memory is thus completely erased from the PDMF. The MF in the inner regions is always significantly flatter than the PDMF as a result of mass segregation.

(iii) The ratio of the total mass of white dwarfs retained in the cluster to the total mass of the cluster, $M_{wd}/M(t)$, increases during the evolution: as the fraction of the initial mass left in the cluster decreases, the fraction of this in white dwarfs increases. The total mass of white dwarfs is determined by the interplay between the rate of production determined by the time scales of stellar evolution and the rate of escape through the tidal boundary of the white dwarfs, or possibly of their progenitors, determined by the relaxation time and disk shocking time scale. We have obtained an analytical expression for the fraction of white dwarfs present in a cluster as a function of the initial conditions and of time as the product of the production rate, that can be easily derived analytically once the IMF has been given, by the escape rate, which is derived instead from a fit to the N-body data. Analogously to what was shown for the difference between the initial and the final slope of the MF, the dependence of $M_{wd}/M(t)$ on $M(t)/M_i$ is the same no matter whether the effects of disk shocking are included or not.

We have made a comparison between our estimate of the fraction of white dwarfs and the one which would be obtained by extrapolating the present day main sequence mass function (a procedure often used in literature) and we have shown that the former is, in most cases, smaller than the latter, with the ratio of the two estimates ranging, in most relevant cases, from about 0.65 to 1 depending on the initial conditions.

(iv) All the simulations we have carried out for our work started with an initial number of particles $N = 4096$. The dependence of our results on N has been checked by an additional set of simulations starting with larger number of particles ($N = 8192$, $N = 16384$). In agreement with the results by Aarseth & Heggie (1997a) we have shown that the scaling of time from N-body units to astrophysical units adopted for $N = 4096$ requires a correction of about 20% when the results are to be used to model systems with values of N relevant for real globular clusters.

ACKNOWLEDGMENTS

We thank Sverre Aarseth for the use of NBODY4 and for especially tailoring it to the needs of this project.
We are most grateful to the referee, whose comments have helped to improve the paper.
This work has been supported by SERC/PPARC under grant number GR/J79461, which funded the GRAPE-4 (HARP) hardware.
EV acknowledges financial support by a ESEP fellowship from The Royal Society and Accademia Nazionale dei Lincei and the hospitality of the Department of Mathematics and Statistics of the University of Edinburgh.

REFERENCES

Aarseth S.J., 1985, in Brackbill J.U., Cohen B.I. eds., Multiple Time Scales. Academic Press, New York, p.377
Aarseth S.J., 1994, in Contopoulos G., Spyrou N.K., Vlahos L. eds., Galactic Dynamics and N-body Simulations, Springer Verlag, p.277
Aarseth, S.J., Heggie, D.C., 1997a, submitted to MNRAS
Aarseth, S.J., Heggie, D.C., 1997b, in preparation
Aguilar L., Hut P., Ostriker J.P., 1988, ApJ, 335, 720
Alexander, D.R.,Brocato E., Cassisi S., Castellani V., Ciacio F., Degl'Innocenti S., 1997, A&A, 317,90
Bahcall J.N., 1984, ApJ, 287, 926
Bahcall J.N., Schmidt M., Soneira R.M., 1982, ApJL, 258, L23
Capaccioli, M., Ortolani, S., Piotto, G., 1991, A&A, 244,298
Capaccioli, M.,Piotto, G., Stiavelli, M., 1993, MNRAS, 261, 819
Chandrasekhar, S., 1942, Principles of Stellar Dynamics. Univ. of Chicago Press, Chicago
Chernoff, D.F., Kochanek, C.S., Shapiro, S.L., 1986, ApJ, 309, 183
Chernoff, D.F., Weinberg, M., 1990, ApJ, 351, 121
D'Antona, F., Mazzitelli, I., 1996, ApJ, 456, 329
Dauphole, B., Geffert, M., Colin, J., Odenkirchen, M., Tucholke, H.J., 1996, A&A, 313, 119
Djorgovski, S., Piotto,G., Capaccioli, M., 1993, AJ, 105, 2148
De Marchi, G., Paresce, F., 1995a, A&A, 304,202
De Marchi, G., Paresce, F., 1995b, A&A, 304,211
Drukier G., 1996, MNRAS, 280, 498
Elson, R., Gilmore, G., Santiago, B., Casertano, S., 1995, AJ, 110,682
Fukushige, T., Heggie, D.C., 1995, MNRAS, 276, 206
Gebhardt K., Pryor C., Williams T.B., Hesser J.E., Stetson P.B., 1997, AJ, 113, 1026
Giersz, M., Heggie, D.C., 1994, MNRAS, 270, 298
Giersz, M., Heggie, D.C., 1997, MNRAS, in press
Gnedin O., Ostriker J.P., 1997, ApJ, 474, 223
Heggie,D.C., Mathieu, R.D., 1986, in Hut P., McMillan, S.L.W. eds., The Use of Supercomputers in Stellar Dynamics. Springer-Verlag, Berlin, p.233
Heggie D.C., Hut P., 1996,in Dynamical Evolution of Star Clusters, IAU Symp. 174, eds. P.Hut and J.Makino, p.303
Hills J.G., 1980, ApJ, 235, 986
Iben I.J., Renzini A., 1983, ARA&A, 21, 271
King, I.R., 1966, AJ, 71, 64
King, I.R., 1996, in Dynamical Evolution of Star Clusters, IAU Symp. 174, eds. P.Hut and J.Makino, p.29
King, I.R., Sosin, C., Cool,A.M., 1995, ApJL, 452, L33
Lada C.J., Margulis M., Dearborn D.S., 1984, ApJ, 285, 141
Makino, J., Kokubo, E., Taiji, M., 1993, PASJ, 45, 349
McClure, R.D.,et al., 1986, ApJ, 307,L49
Meylan, G., 1987, A&A, 184, 144
Paresce, F., De Marchi, G., Romaniello, M., 1995, ApJ, 440, 216
Piotto, G., 1991,in Formation and Evolution of Star Clusters, ed. K.Janes, ASPCS vol.13, p.200
Piotto, G., Cool, A.M., King I.R., 1996, in Dynamical Evolution of Star Clusters, IAU Symp. 174, eds. P.Hut and J.Makino, p.71
Piotto, G., Cool, A.M., King I.R., 1997, AJ, in press
Richer, H.B., Fahlman, G.G., Buonanno, R., Fusi Pecci, F., Searle, L., Thompson, I.B., 1991, ApJ, 381,147
Richer H.B., Fahlman G.G., Ibata R.A., Stetson P.B., Bell R.A., Bolte M., Bond H.E., Harris W.E., Hesser J.E., Mandushev G., Pryor C., Vandenberg D.A., 1995, ApJ, 451, L17

Richer H.B., Fahlman G.G., Ibata R.A.,Pryor C.,Bell R.A., Bolte M., Bond H.E., Harris W.E., Hesser J.E., Holland S., Ivanans N., Mandushev G., Stetson P.B., Wood M.A., 1997, ApJ, submitted

Santiago, B.,Elson, R., Gilmore, G., 1996, MNRAS, 281, 1363

Spitzer, L., 1958, ApJ, 127, 17

Spitzer, L., 1987, Dynamical evolution of globular clusters, Princeton University Press

Stiavelli, M., Piotto, G.,Capaccioli, M., Ortolani, S., 1991,in Formation and Evolution of Star Clusters, ed. K.Janes, ASPCS vol.13, 449

Stiavelli, M., Piotto, G.,Capaccioli, M., 1992, in Morphological and Physical Classification of Galaxies, ed. G.Longo, M.Capaccioli and G. Busarello, p.445

Weinberg, M., 1994, AJ, 108, 1414

Table 1
Results of the simulations including two-body relaxation and stellar evolution

$M_i(M_\odot)$	R_g (Kpc)	$F_{cw}/10^4$	W_0	α_i	M_f/M_i	M_{wd}/M_f	α_f	$\alpha_i - \alpha_f$
6.15×10^4	4	2.0	7	2.5	0.205	0.279	1.46	1.04
6.15×10^4	5	2.5	7	2.5	0.307	0.199	1.81	0.69
6.15×10^4	8	4.0	7	2.5	0.524	0.149	2.21	0.29
6.15×10^4	16	8.0	7	2.5	0.657	0.128	2.41	0.09
6.15×10^4	4	2.0	5	2.5	0.195	0.273	1.38	1.12
6.15×10^4	5	2.5	5	2.5	0.344	0.196	1.96	0.54
6.15×10^4	8	4.0	5	2.5	0.542	0.150	2.31	0.19
6.15×10^4	16	8.0	5	2.5	0.670	0.130	2.39	0.11
6.15×10^4	4	1.92	7	3.5	0.633	0.013	3.27	0.23
6.15×10^4	5	2.4	7	3.5	0.702	0.012	3.39	0.11
6.15×10^4	8	3.84	7	3.5	0.808	0.014	3.42	0.08
6.15×10^4	16	7.68	7	3.5	0.890	0.019	3.46	0.04

Final values are calculated at $t = 15$ Gyr
M_{wd} is the total mass of white dwarfs in the cluster at $t = 15$ Gyr.

Table 2
Results of simulations including two-body relaxation, stellar evolution and disk shocking

$M_i(M_\odot)$	R_g (Kpc)	$F_{cw}/10^4$	M_f/M_i	M_{wd}/M_f	α_f	$\alpha_i - \alpha_f$	$\Delta\alpha_{ds}$	$\Delta M_{ds}/M_i$
6.15×10^4	4	2.0	0.080	0.340	0.37	2.13	1.05	0.113
6.15×10^4	5	2.5	0.254	0.242	1.50	1.00	0.39	0.064
6.15×10^4	8	4.0	0.489	0.149	2.18	0.32	0.04	0.015
6.15×10^4	16	8.0	0.670	0.127	2.38	0.12	0.002	-0.011
1.59×10^5	2.1	2.5	0.166	0.292	1.12	1.38	0.77	0.156
1.59×10^5	3.3	4.0	0.418	0.168	2.10	0.40	0.11	0.083
1.59×10^5	6.7	8.0	0.610	0.123	2.35	0.15	0.03	0.050
4.79×10^4	5	1.99	0.082	0.357	0.39	2.11	0.99	0.107
7.59×10^4	5	3.03	0.337	0.179	1.91	0.59	0.16	0.068
8.99×10^4	5	3.5	0.391	0.176	2.02	0.48	0.14	0.073
1.12×10^5	5	4.3	0.471	0.148	2.13	0.37	0.12	0.057
1.58×10^5	5	5.99	0.563	0.142	2.30	0.20	0.03	0.043
3.16×10^5	5	11.3	0.658	0.127	2.40	0.10	0.02	0.047
1.99×10^4	14.0	2.5	0.345	0.195	1.95	0.55	-0.07	-0.029
3.16×10^4	9.2	2.5	0.323	0.210	1.85	0.65	0.03	-0.006
3.98×10^4	7.45	2.5	0.266	0.222	1.64	0.86	0.24	0.051
7.94×10^4	3.95	2.5	0.233	0.255	1.53	0.97	0.35	0.084
1.00×10^5	3.2	2.5	0.191	0.257	1.53	0.97	0.35	0.127
3.16×10^5	1.1	2.5	0.173	0.289	1.25	1.25	0.63	0.143

All the systems have initially $W_0 = 7$ and $\alpha_i = 2.5$
Final values are calculated at $t = 15$ Gyr

Table 3

id	N	M_f/M_i	M_{wd}/M_f	α_f	t_{cc}(Gyr)
I	4096	0.195	0.273	1.38	6.0
II	4096	0.242	0.268	1.50	7.5
III	4096	0.195	0.281	1.44	5.5
IV	4096	0.202	0.286	1.32	7.1
I	8192	0.127	0.365	0.86	6.3
II	8192	0.156	0.325	1.25	6.9
I	16384	0.075	0.422	0.54	7.6

Disk shocking is not included in these simulations.
Final values are calculated at $t = 15$ Gyr.
Initial conditions:
$W_0 = 5,\ \alpha_i = 2.5,\ R_g = 4\mathrm{Kpc},\ M_i = 6.15 \times 10^4 M_\odot$
t_{cc} is the time of core collapse

FIGURE CAPTIONS

Figure 1 Time evolution of the main properties of systems starting with $\alpha_i = 2.5$, $W_0 = 7$, $M_i = 6.15 \times 10^4 M_\odot$ and having galactocentric distances equal to $R_g = 4$ Kpc (solid line), $R_g = 5$ Kpc (dotted line), $R_g = 8$ Kpc (short-dashed line), $R_g = 16$ Kpc (long-dashed line). (a) Evolution of the total number of stars;(b) evolution of the ratio of total mass to initial mass; (c) evolution of the total number of stars having a mass in the range $0.1 - 0.12\ m_\odot$ (upper curves) and $0.25 - 0.31\ m_\odot$ (lower curves) for the systems located at $R_g = 4$ Kpc (solid lines) and at $R_g = 16$ Kpc (long-dashed lines); (d) evolution of the ratio of the total mass of neutron stars to the total mass at time t; (e) evolution of the ratio of total mass of white dwarfs to the total mass at time t; (f) Evolution of the slope of the mass function calculated for main sequence stars in the range $0.1 < m/m_\odot < 0.5$.

Figure 2 Time evolution of the mass function for main sequence stars for the system with $\alpha_i = 2.5$, $W_0 = 7$, $M_i = 6.15 \times 10^4 M_\odot$ and $R_g = 4$ Kpc. The four curves shown correspond (from the upper to the lower one) to $t = 0$ Gyr, $t = 7$ Gyr, $t = 10$ Gyr, $t = 15$ Gyr.

Figure 3 (a) Time evolution of the ratio of total mass to initial mass for systems with $\alpha_i = 2.5$, $W_0 = 7$, $M_i = 6.15 \times 10^4 M_\odot$ and $R_g = 4, 5, 8, 16$ Kpc (symbols as in Figure 1). Straight lines take into account only the mass loss by relaxation, curved lines only the mass loss by stellar evolution. The latter curve does not depend significantly on the galactocentric distance of the system and the four curves are almost indistinguishable; (b) evolution of the ratio of total mass to initial mass for systems with $\alpha_i = 2.5$, $W_0 = 7$, $M_i = 6.15 \times 10^4 M_\odot$ and $R_g = 4, 5, 8, 16$ Kpc (symbols as in Figure 1) including only the mass loss by relaxation versus time scaled by the value of F_{cw} for each system.

Figure 4 (a) Fraction of the initial mass remaining in a cluster after 15 Gyr, $M(15\text{Gyr})/M_i$, as a function of $\log M_i$ and R_g for systems with $\alpha_i = 2.5$ and $W_0 = 7$; (b) contours of constant values of $M(15\text{Gyr})/M_i$, as indicated on the right end of the curves shown in the plot, as a function of the galactocentric distance and of the logarithm of the initial mass.

Figure 5 Slope of the mass function at $t = 15$ Gyr measured for main sequence stars with masses in the range $m = [0.1, 0.5]\ m_\odot$ from the analytic expression derived in the text (see eq.(16)) as a function of galactocentric distance for the following values of the initial mass of the cluster (from the upper to the lower curve): $\log M_i = 6, 5.5, 5.2, 5, 4.79, 4.5$. Initial conditions are $\alpha_i = 2.5$, $W_0 = 7$. Dots represent values obtained from N-body simulations for $\log M_i = 4.79$.

Figure 6 Time evolution of the slope of the mass function of main sequence stars with $0.1 < m/m_\odot < 0.5$ calculated in three different 3-d and 2-d shells (see text for their exact limits): data for the innermost shell are plotted by a solid line and circles, for the intermediate shell by short-dashed line and triangles, for the outermost shell by long-dashed line and crosses.

Initial conditions are $\alpha_i = 2.5$,$W_0 = 7$, $M_i = 6.15 \times 10^4 M_\odot$ and galactocentric distance as indicated below. (a) 3-d shells, $R_g = 4$ Kpc; (b) 2-d shells, $R_g = 4$ Kpc; (c) 3-d shells, $R_g = 16$ Kpc; (d) 2-d shells, $R_g = 16$ Kpc.

Figure 7 (a) Evolution of the difference between the slope of the mass function in 3-d shells and the slope of the initial mass function (all measured for main sequence stars with $0.1 < m/m_\odot < 0.5$) for the system at $R_g = 4$ Kpc. Initial conditions of the systems: $W_0 = 7$, $\alpha_i = 2.5$, $M_i = 6.15 \times 10^4\ M_\odot$. (b) Evolution of the difference between the slope of the mass function in 3-d shells and the slope of the global mass function at time t (all measured for main sequence stars with $0.1 < m/m_\odot < 0.5$) for the system at $R_g = 4$ Kpc.

(c)-(d) same as (a) and (b) but for the system at $R_g = 16$ Kpc. Symbols as in figure 6.

Figure 8 (a) Time evolution of the ratio of total mass in white dwarfs at time t to the total initial mass for systems with $\alpha_i = 2.5$, $W_0 = 7$, $M_i = 6.15 \times 10^4\ M_\odot$ and $R_g = 4$ Kpc (solid line), 5 Kpc (dotted line), 8 Kpc (short-dashed line), 16 Kpc (long-dashed line). The dot-dashed line is the fraction of total mass in white dwarfs expected if all the white dwarfs produced were retained in the cluster and none escaped due to relaxation (see eq.(19) in the text), $M_{wd,prod}$.

(b) Ratio of the total mass of white dwarfs retained in a system at time t to the total mass of white dwarfs actually produced for systems with $\alpha_i = 2.5$, $W_0 = 7$, $M_i = 6.15 \times 10^4 M_\odot$ and $R_g = 4$ Kpc (solid line), 5 Kpc (dotted line), 8 Kpc (short-dashed line), 16 Kpc (long-dashed line) versus time.

(c) Same as (b) but with time scaled by the parameter F_{cw}. Data from runs with $W_0 = 5$ are also shown in this plot. (symbols distinguishing different R_g as in (b)).

(d) Ratio of total mass in white dwarfs at time t to the total mass of white dwarfs produced at time t versus t/F_{cw} (average values of the two runs starting $W_0 = 5$ and $W_0 = 7$ both with $\alpha_i = 2.5$, $R_g = 4$ Kpc, $M_i = 6.15 \times 10^4 M_\odot$). The line superimposed is the result of a polynomial fit (see eq.(21) in the text).

Figure 9 Fraction of the total mass at $t = 15$ Gyr in white dwarfs as a function of the parameter F_{cw} calculated by eq.(20) (see text).

Figure 10 Fraction of the total mass at $t = 15$ Gyr in white dwarfs as a function of $\log M(15\text{ Gyr})$ at different distances from the galactic center (calculated by eq.(20) in the text).

Figure 11 In all figures dashed lines show the time evolution of the slope of the mass function for clusters with (from the lower to the upper curve) $F_{cw} = 20000, 25000, 40000, 80000$ calculated by eq.(16) in the text.

(a) Contours of equal values of $M_{wd}(t)/M(t)$ as a function of time, t, and slope of the mass function at time t calculated according to eq.(20) in the text taking $\alpha_i = 2.5$ and $W_0 = 7$.

(b) Contours of equal values of $M_{wd}(t)/M(t)$ as a function of time, t, and slope of the mass function at time t calculated by extrapolating the current properties of a cluster back in time ("observational" procedure; see text for further details). (c)Contours of equal values of the ratio of the theoretical estimate of $M_{wd}(t)/M(t)$ to the "observational" one as a function of time, t, and slope of the mass function at time t.
Figure 12 As in figure 11 but as a function of the logarithm of the mass of the cluster at $t = 15$ Gyr and of its galactocentric distance.
Figure 13 Same as figure 5 with arrows showing the additional change in the slope of the mass function due to the effects of disk shocking (data from N-body simulations).
Figure 14 (a) Comparison of the time evolution of $M(t)/M_i$ for systems with the effects of disk shocking and without them. All the systems start with $\alpha_i = 2.5$ and $W_0 = 7$, $M_i = 6.15 \times 10^4 M_\odot$; galactocentric distances are $R_g = 4, 5, 8, 16$ Kpc (solid,dotted,short-dashed and long-dashed line respectively).For each pair the lower curve is the one relative to the run with disk shocking, with the exception of the runs at $R_g = 16$ Kpc for which the lower one refers to the run without disk shocking. (b) Same as (a) for the evolution of the slope of the mass function.
Figure 15 Fraction of the total mass at $t = 15$ Gyr in white dwarfs as a function of the fraction of the initial mass left in the cluster at $t = 15$ Gyr. Solid line is calculated by the analytical expression (eq.(20)) derived in the text. Dots are data from N-body simulations with $\alpha_i = 2.5$ (full dots from runs without disk shocking, see Table 1 and Table 3; circles from runs with disk shocking, see Table 2; triangles from runs starting with $N = 8192$ and the cross refers to the run with $N = 16384$ see Table 3).
Figure 16 Difference between the initial value of the slope of the mass function ($\alpha_i = 2.5$) and its value at $t = 15$ Gyr as a function of the fraction of the initial mass left in the cluster at $t = 15$ Gyr. Solid line is calculated by the analytical expression (eq.(16)) derived in the text. Dots are data from N-body simulations (symbols as in figure 15).
Figure 17 Time evolution of the ratio of mass at time t to initial mass not considering mass loss due to stellar evolution for four runs with disk shocking. Straight lines show the best linear fit of the curves obtained from N-body data. From the lower to the upper one , the curves refer to the following initial conditions $\log M_i = 4.68,\ R_g = 5$ Kpc , $\log M_i = 5.5,\ R_g = 1.1$ Kpc, $\log M_i = 4.3,\ R_g = 14$ Kpc, $\log M_i = 5.5,\ R_g = 5$ Kpc.
Figure 18 Slope of $M(t)/M_i$ (not taking into account mass loss by stellar evolution) for runs with disk shocking from N-body data versus the analytical expression derived in the text (see eq.(23)). The line is given by λ(N-body) = λ(fit).
Figure 19 (a) $M(15\mathrm{Gyr})/M_i$ versus the parameter F_{cw} for runs with (circles) and without (full dots) disk shocking. Solid line is calculated by the analytical expression derived in the text (eq.(11)). (b) Same as (a) but with the family parameter F_{cw} replaced by the equivalent family parameter F_{cw}^{eq} defined in the text.
Figure 20 Contours of equal values (given at the right side of each pair of curves) of the family parameter F_{cw} (solid lines) and of the equivalent family parameter, F_{cw}^{eq}, defined in the text.
Figure 21 Contours of equal values of the mass of a cluster at $t = 15$ Gyr with (dashed lines) and without (solid lines) the effects of disk shocking; initial conditions $W_0 = 7$ and $\alpha_i = 2.5$. The number beside each curve gives $\log M(15\mathrm{Gyr})$.
Figure 22 Slope of the mass function at $t = 15$ Gyr for main sequence stars with masses in the range $m = [0.1, 0.5]\ m_\odot$ without (solid lines) and with (dashed lines) the effects of disk shocking calculated by the analytic expression derived in the text (eq.(16) with F_{cw} replaced by F_{cw}^{eq} for the case with disk shocking) as a function of galactocentric distance for the following values of the initial mass of the cluster (from the upper to the lower curve): $\log M_i = 6, 5.5, 5.2, 5, 4.79, 4.5$. Initial conditions are $\alpha_i = 2.5$, $W_0 = 7$.
Figure 23 Slope of $M(t/F_{cw})/M_i$ for systems starting with $W_0 = 5,\ R_g = 4$ Kpc$, \alpha_i = 2.5$ and $M_i = 6.15 \times 10^4 M_\odot$ versus the initial number of stars in the simulation N. Disk shocking was not included in these runs. Four runs have been done for $N = 4096$ and two runs for $N = 8192$.

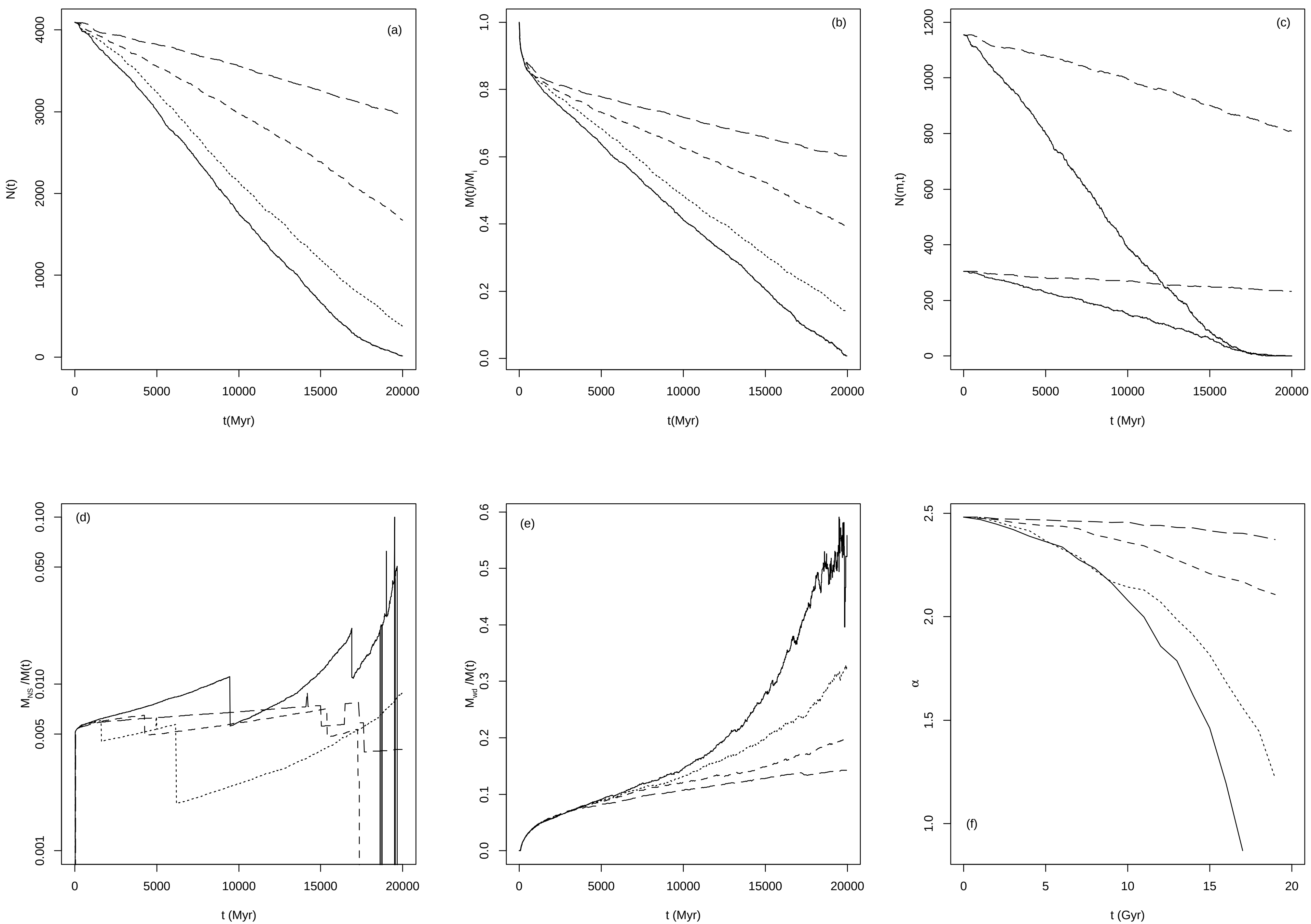
(a)
N(t)
t(Myr)
(b)
M(t)/M_i
t(Myr)
(c)
N(m,t)
t (Myr)
(d)
M_NS /M(t)
t (Myr)
(e)
M_wd /M(t)
t (Myr)
(f)
α
t (Gyr)

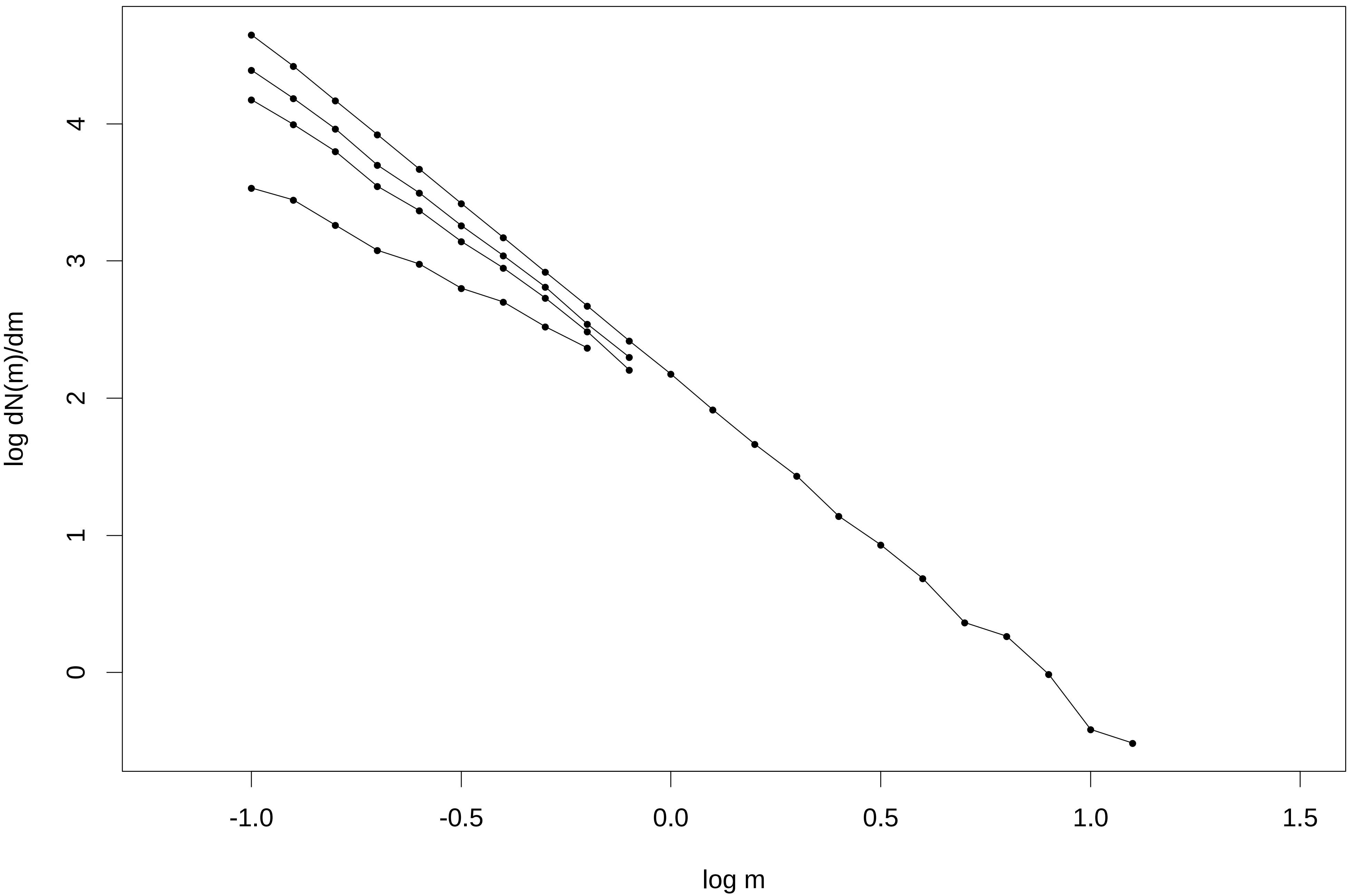
log dN(m)/dm
0
1
2
3
4
-1.0
-0.5
0.0
0.5
1.0
1.5
log m

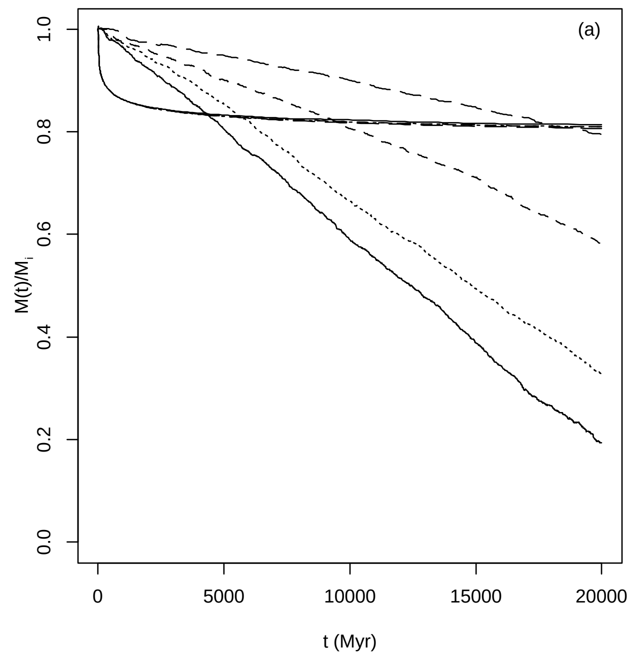

(a)
M(t)/M$_i$
1.0
0.8
0.6
0.4
0.2
0.0
0
5000
10000
15000
20000
t (Myr)

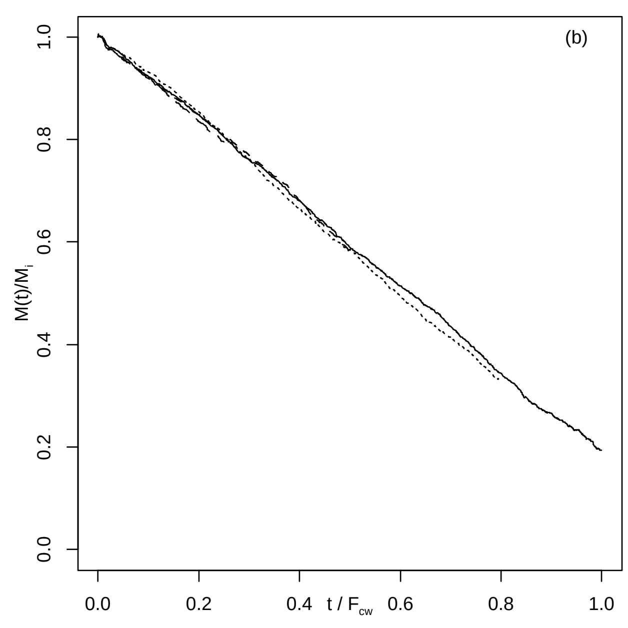

(b)
M(t)/M$_i$
1.0
0.8
0.6
0.4
0.2
0.0
0.0
0.2
0.4
t / F_{cw}
0.6
0.8
1.0

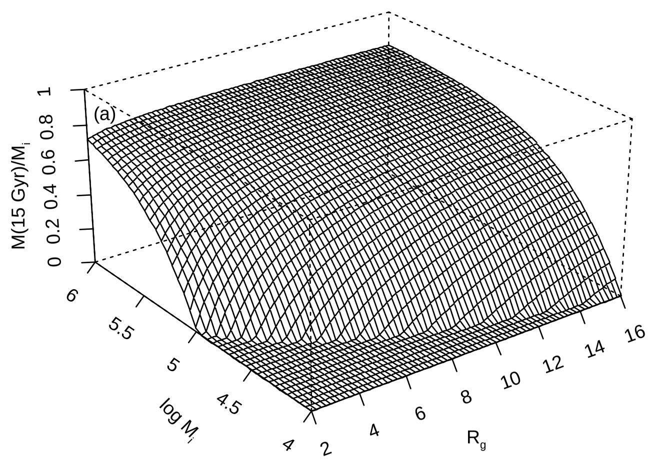
(a)
M(15 Gyr)/M_i
0
0.2
0.4
0.6
0.8
1
6
5.5
5
4.5
4
log M_i
2
4
6
8
10
12
14
16
R_g

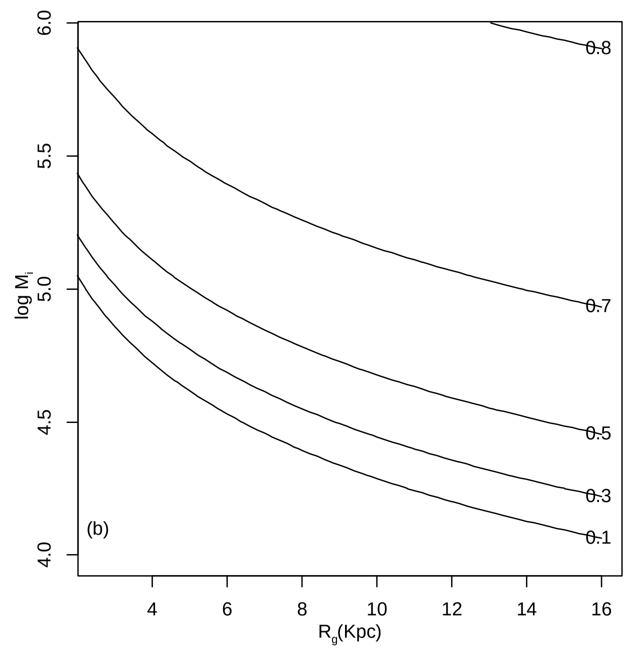
(b)
0.8
0.7
0.5
0.3
0.1
log M_i
4.0
4.5
5.0
5.5
6.0
4
6
8
10
12
14
16
R_g(Kpc)

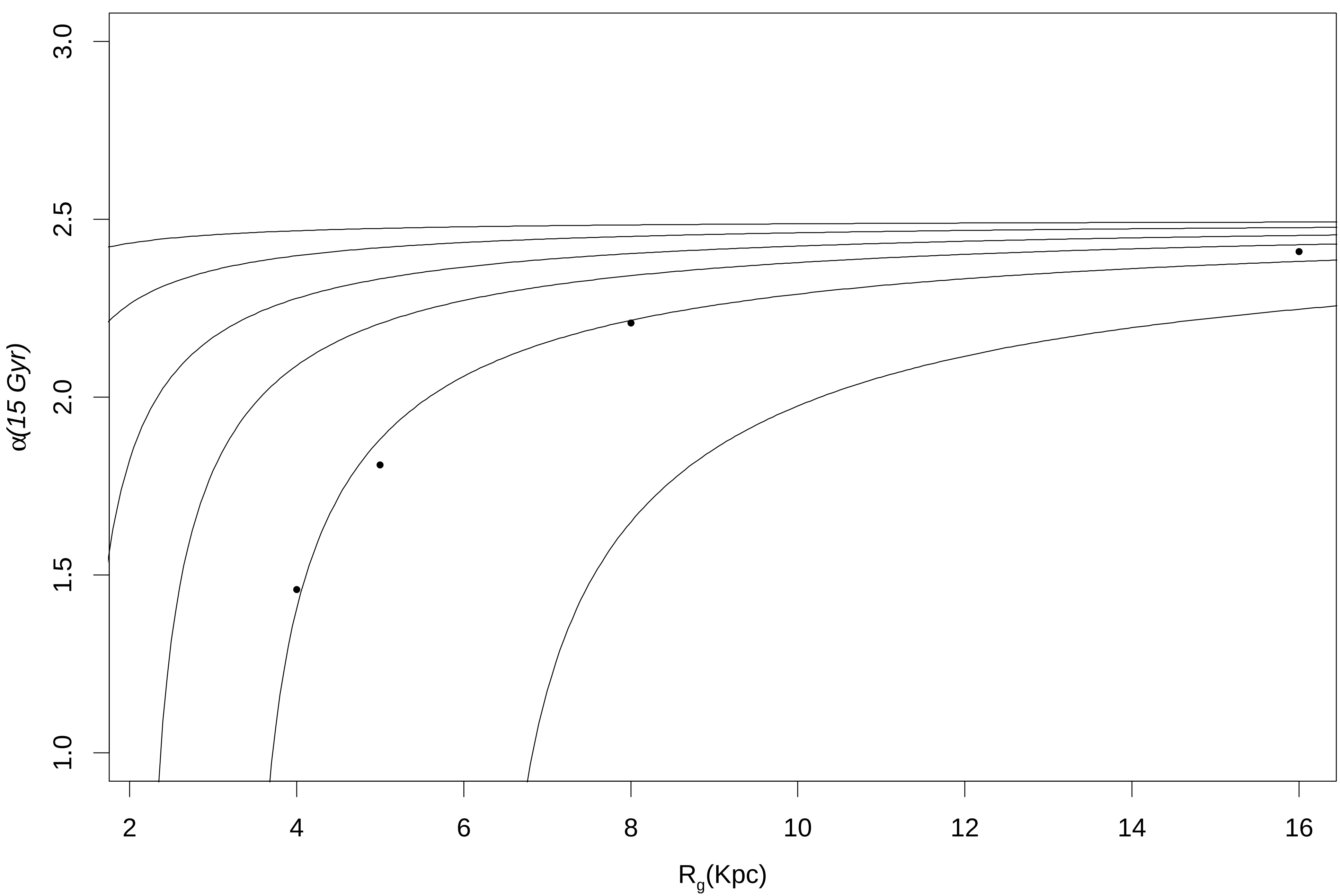

3.0
2.5
2.0
1.5
1.0
α(15 Gyr)
2
4
6
8
10
12
14
16
R_g(Kpc)

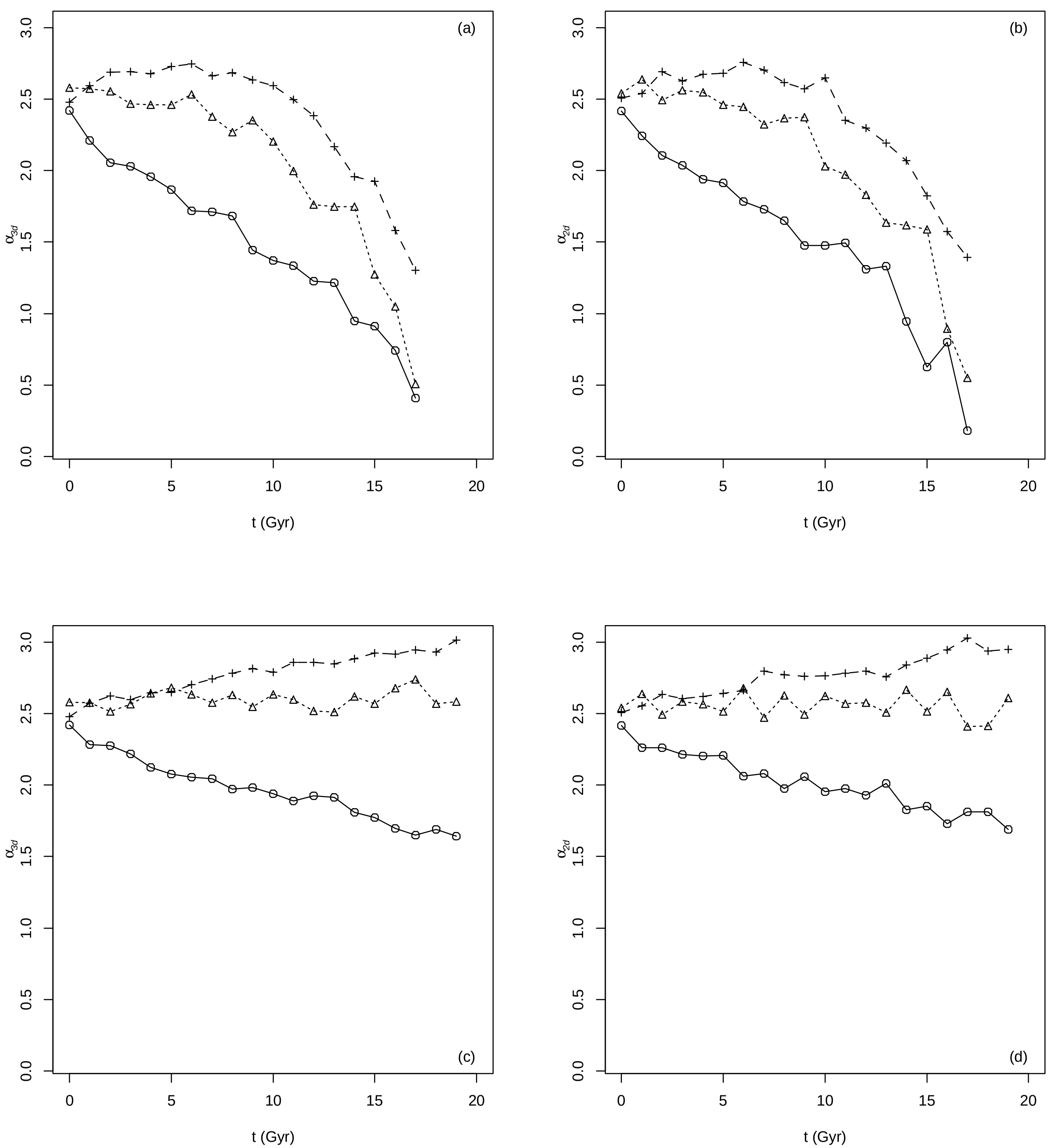

(a)
(b)
(c)
(d)
α_{3d}
α_{2d}
t (Gyr)

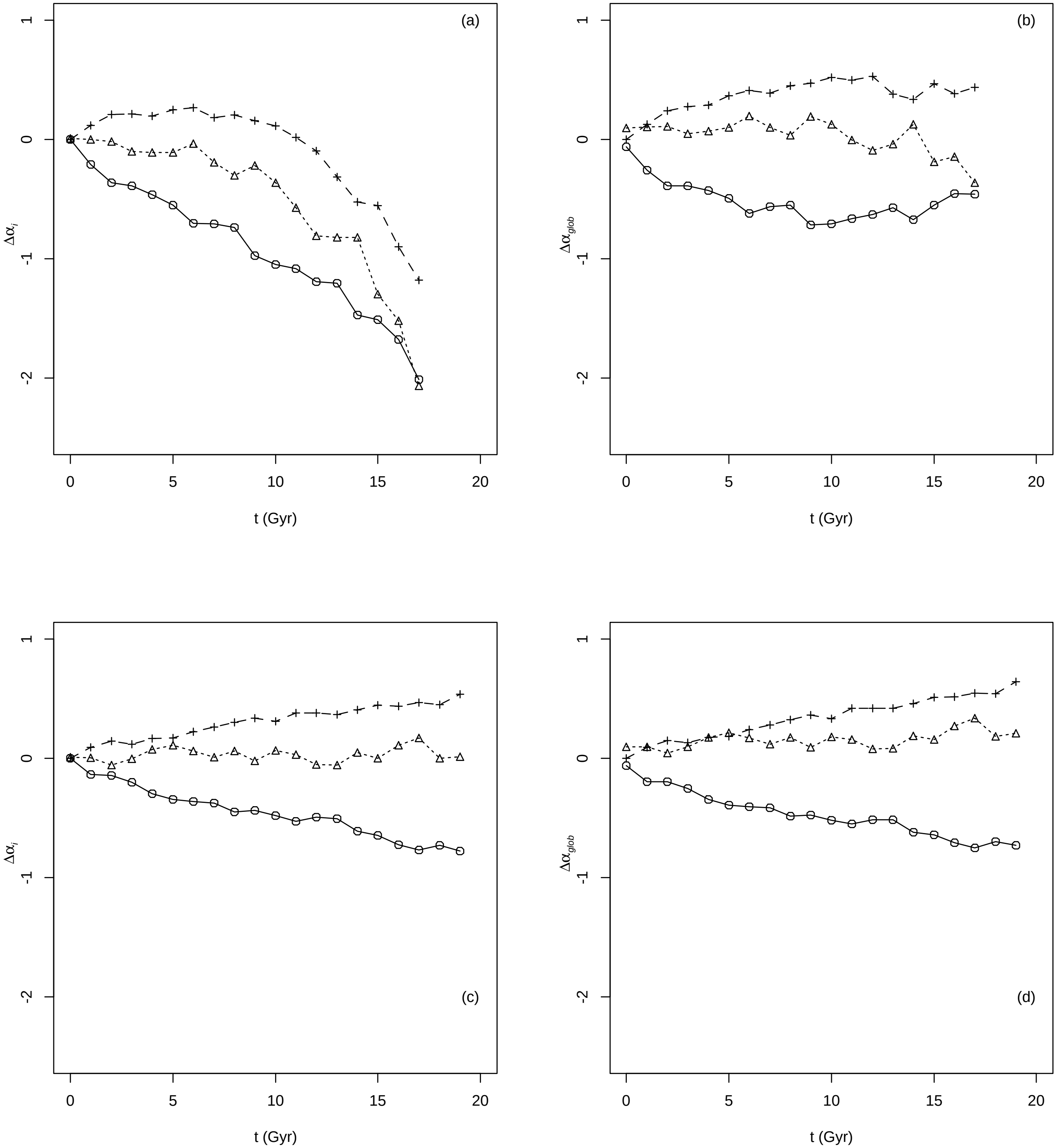

(a)
(b)
(c)
(d)
$\Delta\alpha_i$
$\Delta\alpha_{glob}$
t (Gyr)

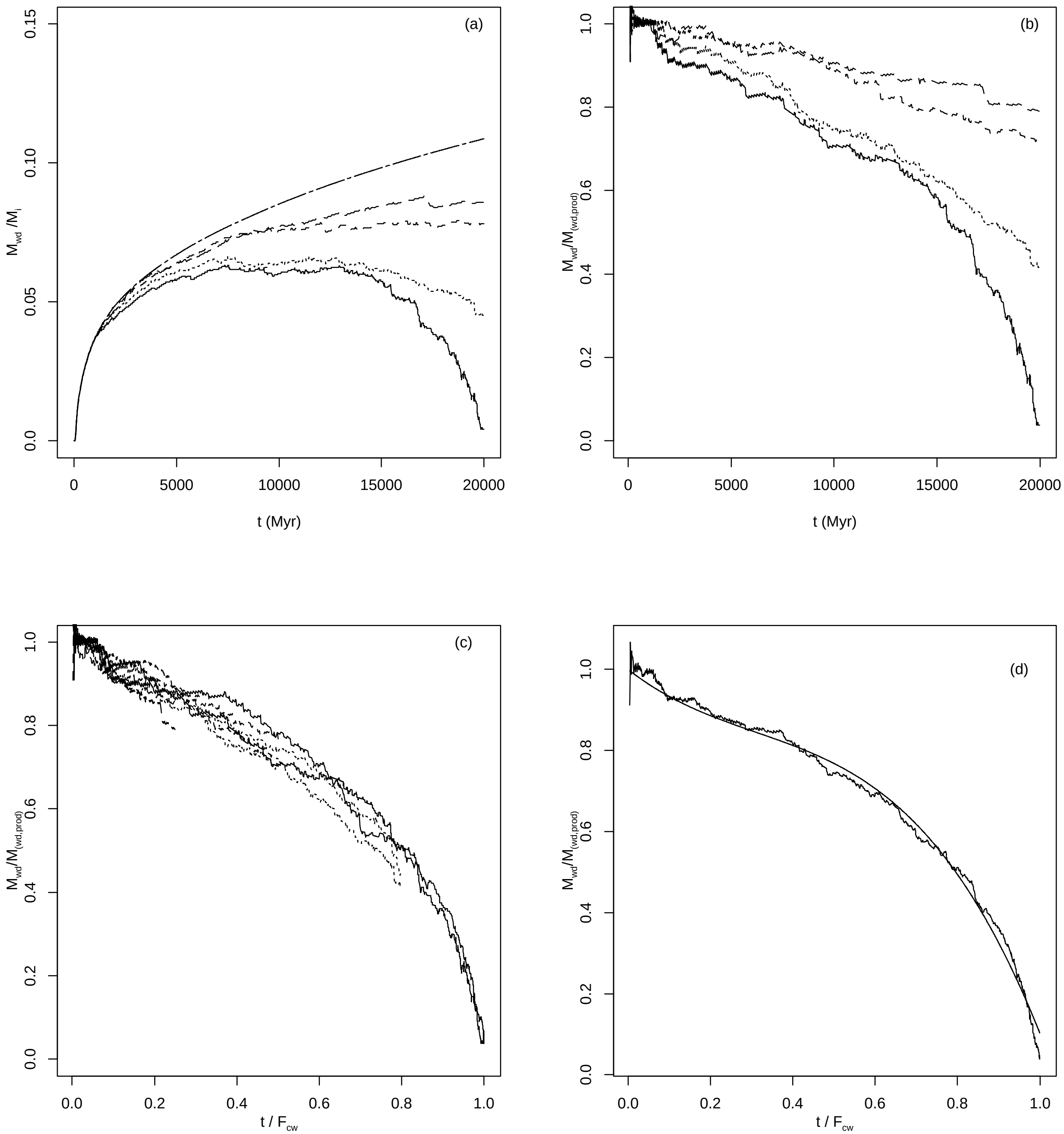
(a)
(b)
(c)
(d)
M_{wd}/M_i
$M_{wd}/M_{(wd,prod)}$
t (Myr)
t / F_{cw}

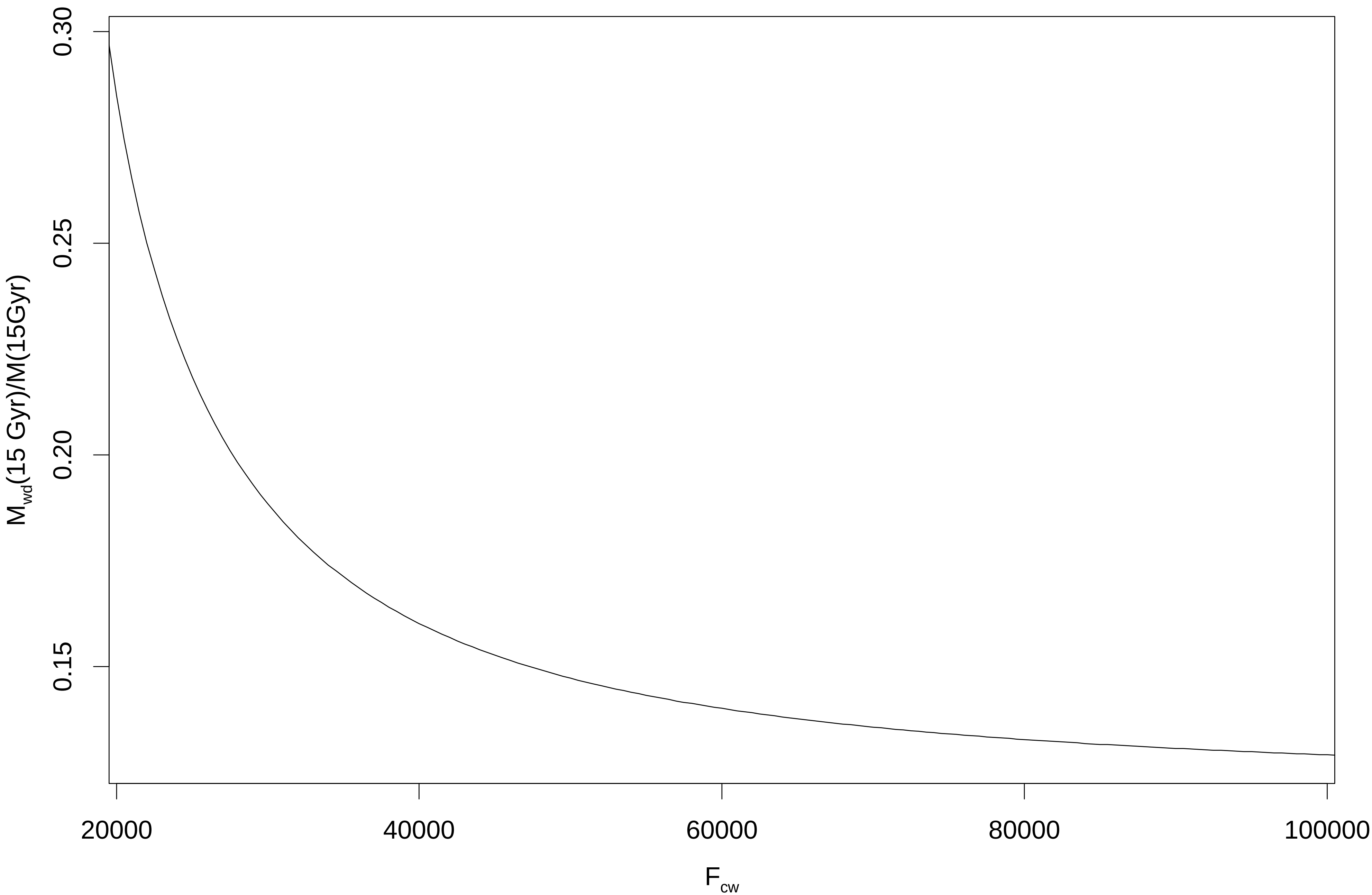
0.30
0.25
0.20
0.15
M_wd(15 Gyr)/M(15Gyr)
20000
40000
60000
80000
100000
F_cw

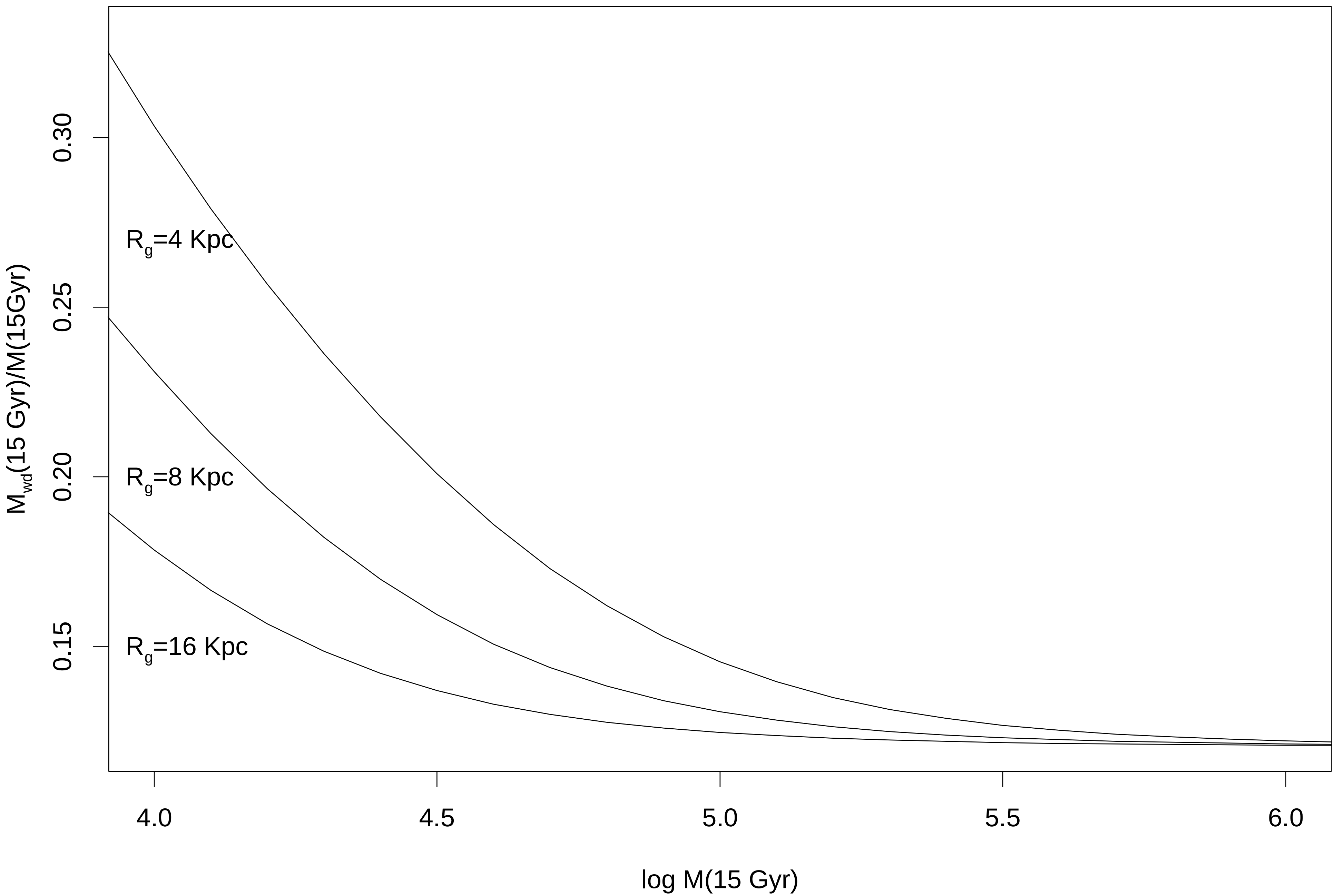

R_g=4 Kpc
R_g=8 Kpc
R_g=16 Kpc
0.15
0.20
0.25
0.30
M_wd(15 Gyr)/M(15Gyr)
4.0
4.5
5.0
5.5
6.0
log M(15 Gyr)

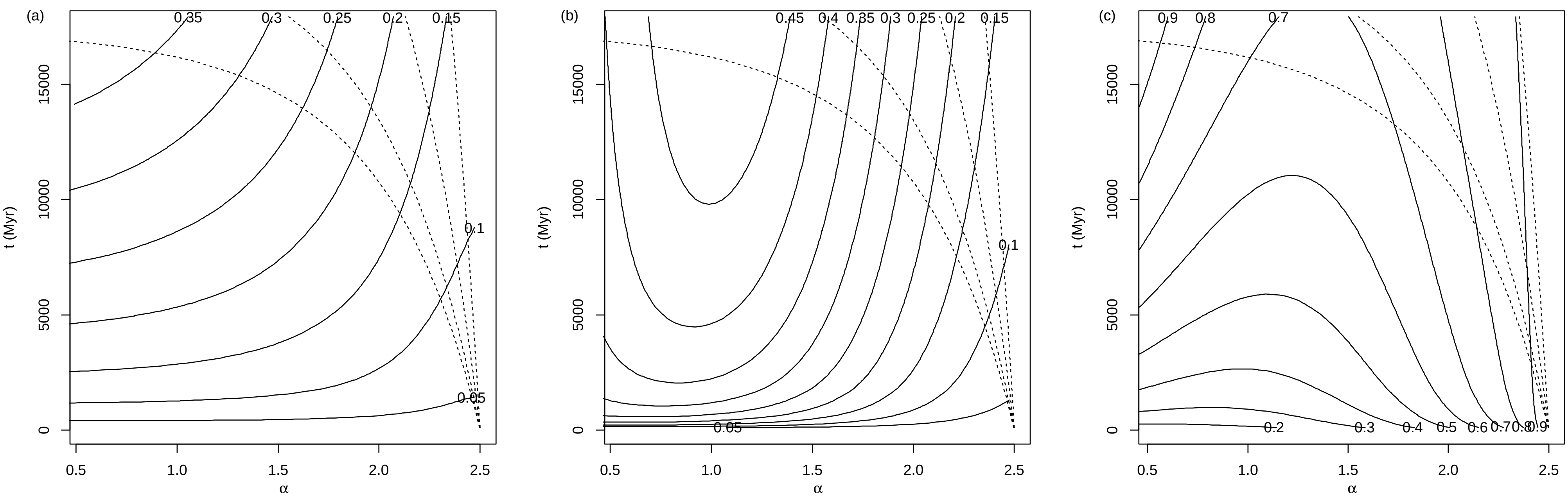

(a)
(b)
(c)
t (Myr)
α
0.35
0.3
0.25
0.2
0.15
0.1
0.05
0.45
0.4
0.9
0.8
0.7
0.6
0.5

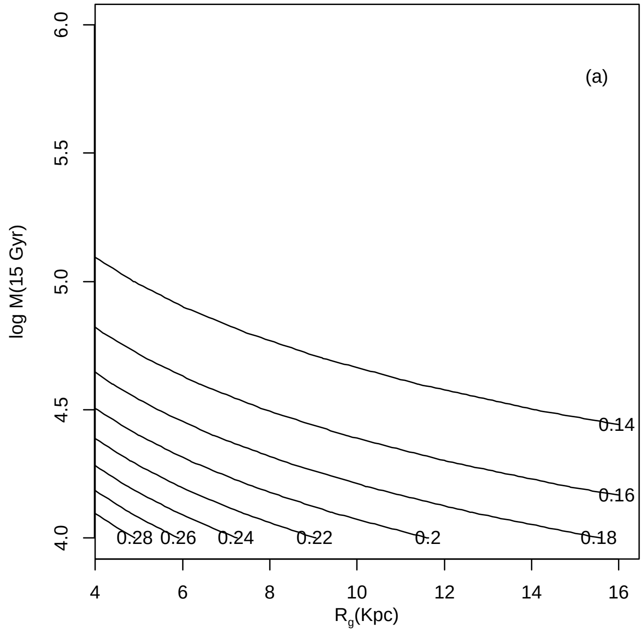

(a)
log M(15 Gyr)
6.0
5.5
5.0
4.5
4.0
0.14
0.16
0.18
0.2
0.22
0.24
0.26
0.28
4
6
8
10
12
14
16
R_g(Kpc)

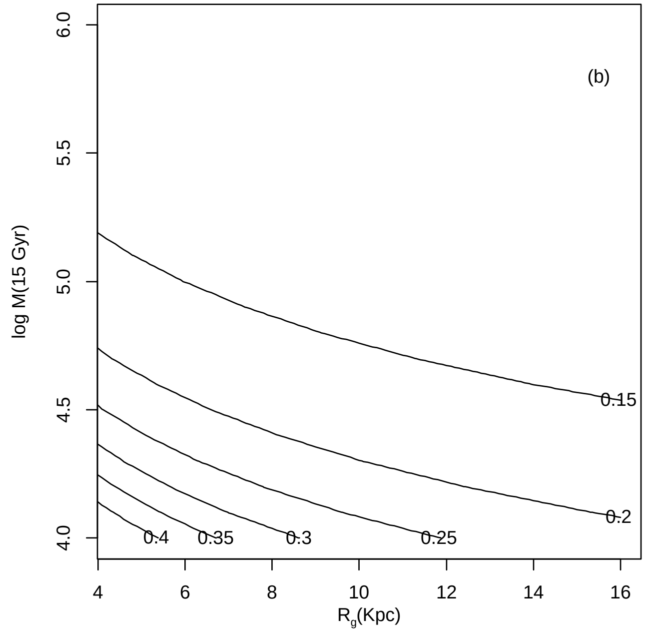

(b)
log M(15 Gyr)
6.0
5.5
5.0
4.5
4.0
0.15
0.2
0.25
0.3
0.35
0.4
4
6
8
10
12
14
16
R_g(Kpc)

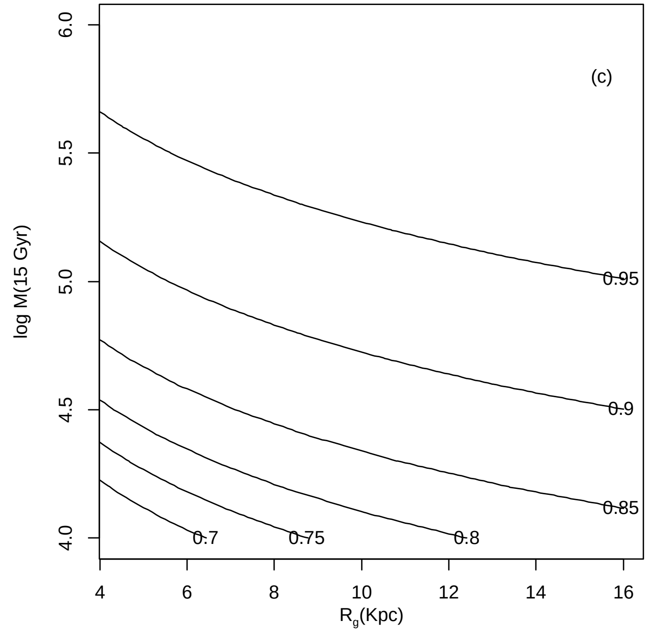

(c)
log M(15 Gyr)
6.0
5.5
5.0
4.5
4.0
0.95
0.9
0.85
0.8
0.75
0.7
4
6
8
10
12
14
16
R_g(Kpc)

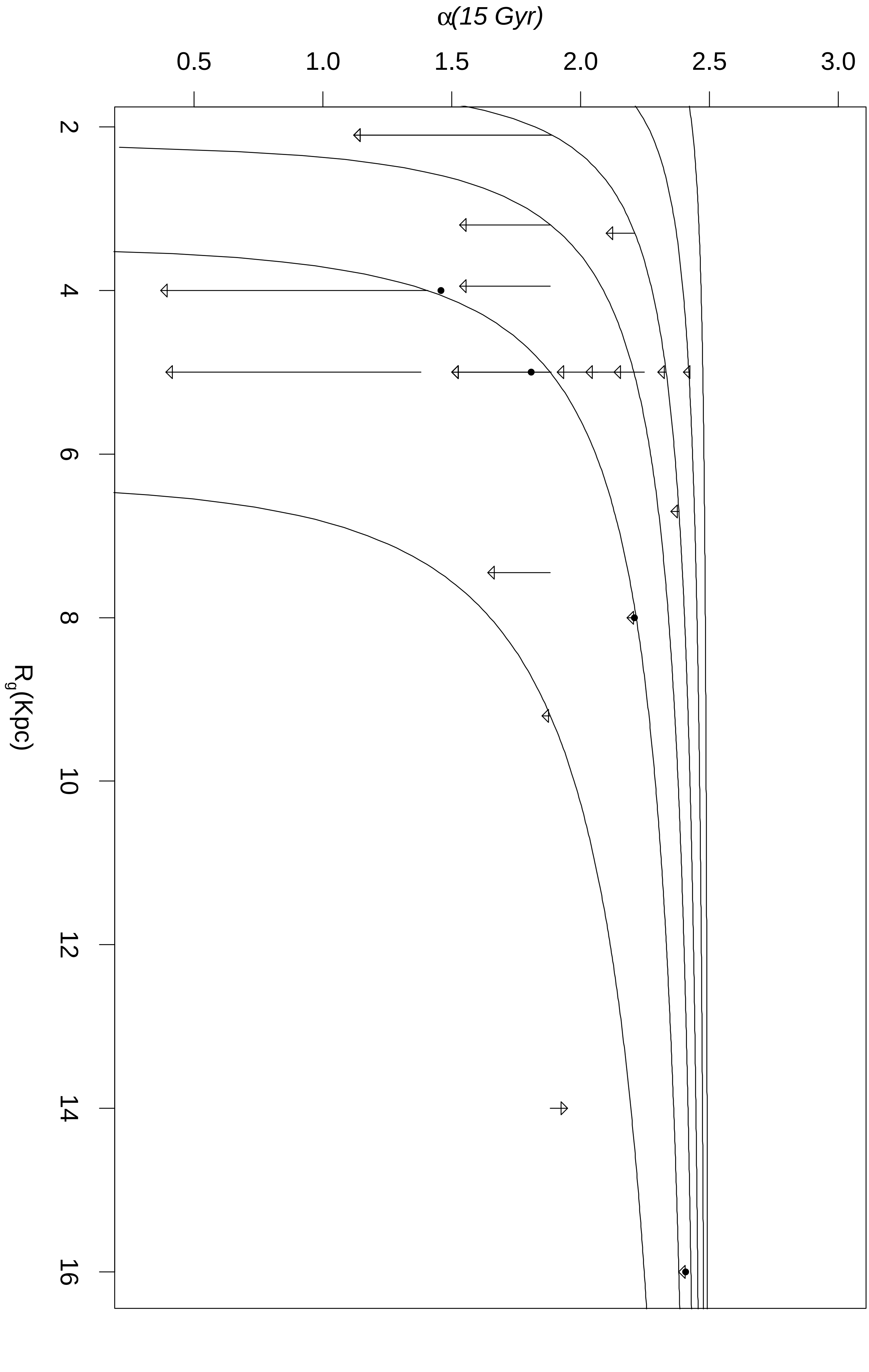
α(15 Gyr)
0.5
1.0
1.5
2.0
2.5
3.0
Rg(Kpc)
2
4
6
8
10
12
14
16

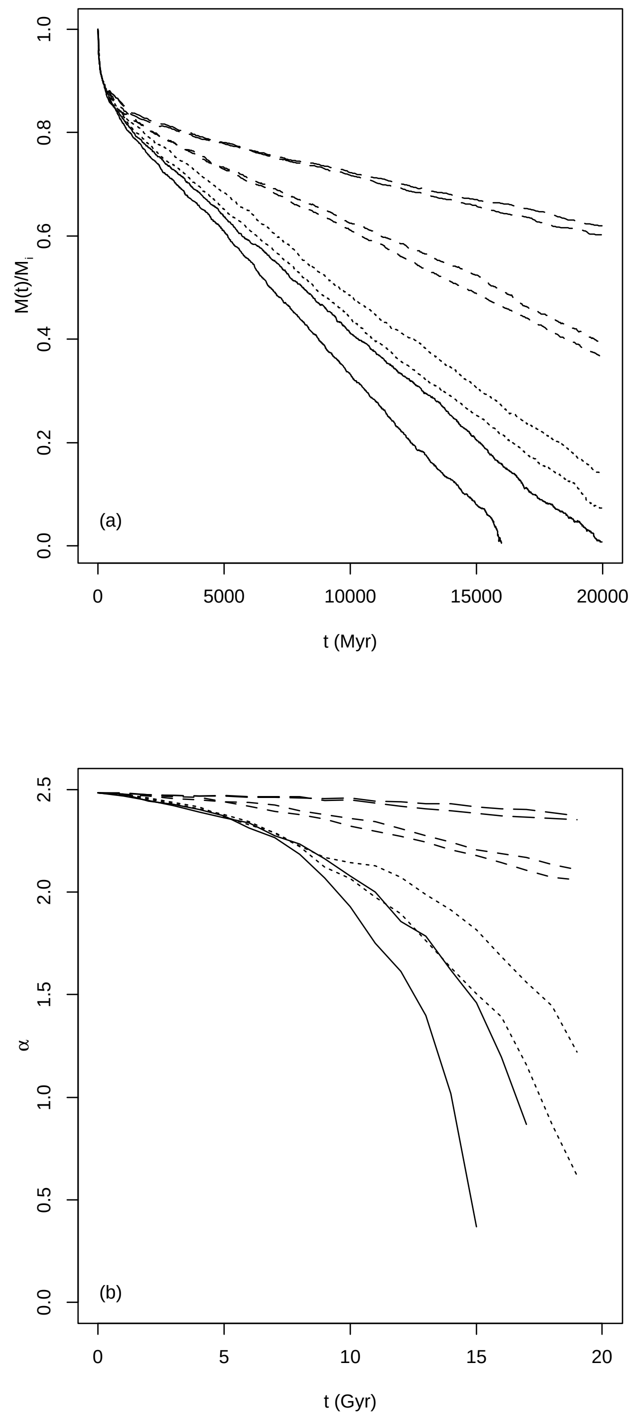

M(t)/M_i
1.0
0.8
0.6
0.4
0.2
0.0
(a)
0
5000
10000
15000
20000
t (Myr)
α
2.5
2.0
1.5
1.0
0.5
0.0
(b)
0
5
10
15
20
t (Gyr)

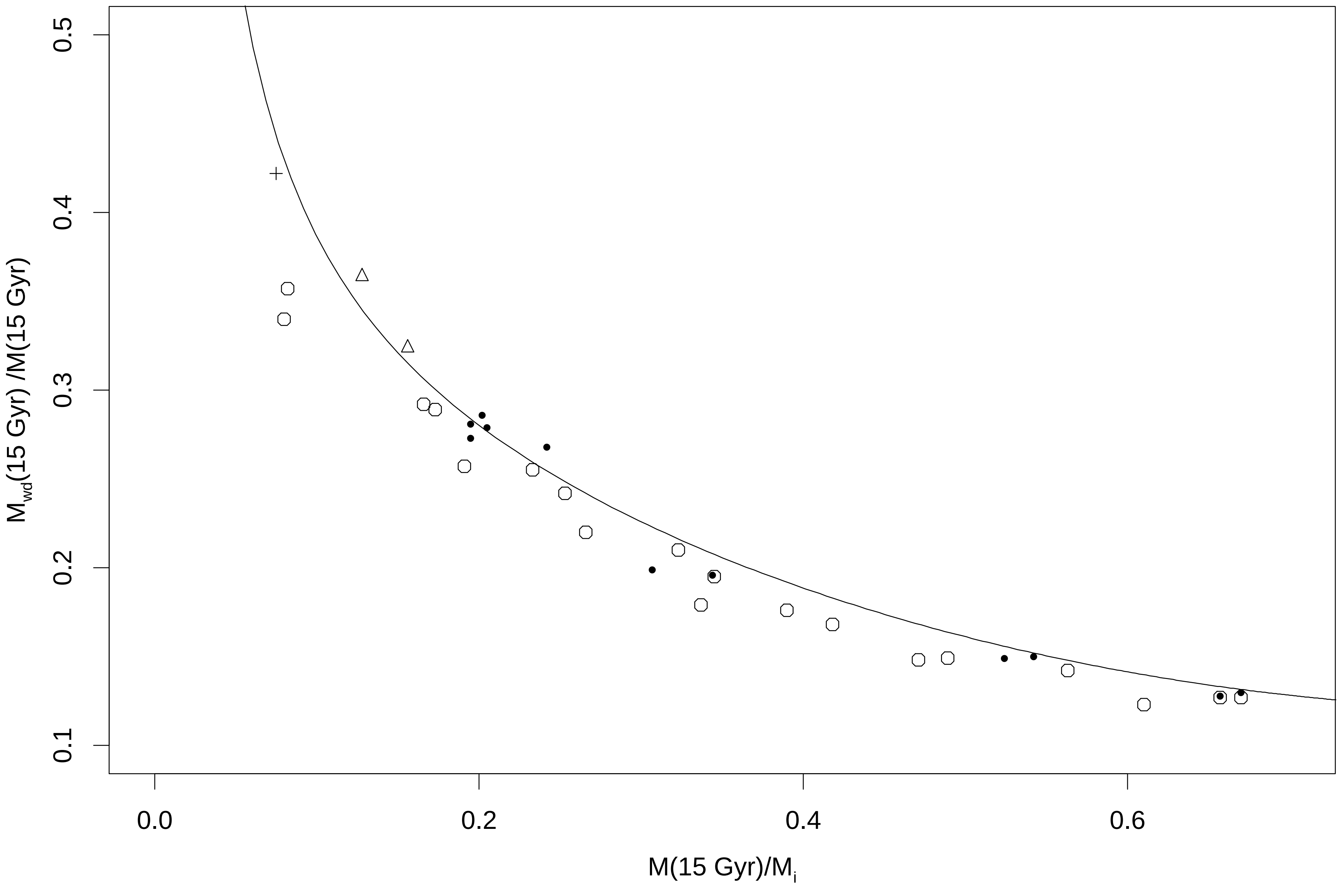

0.1
0.2
0.3
0.4
0.5
M_{wd}(15 Gyr) /M(15 Gyr)
0.0
0.2
0.4
0.6
M(15 Gyr)/M_i

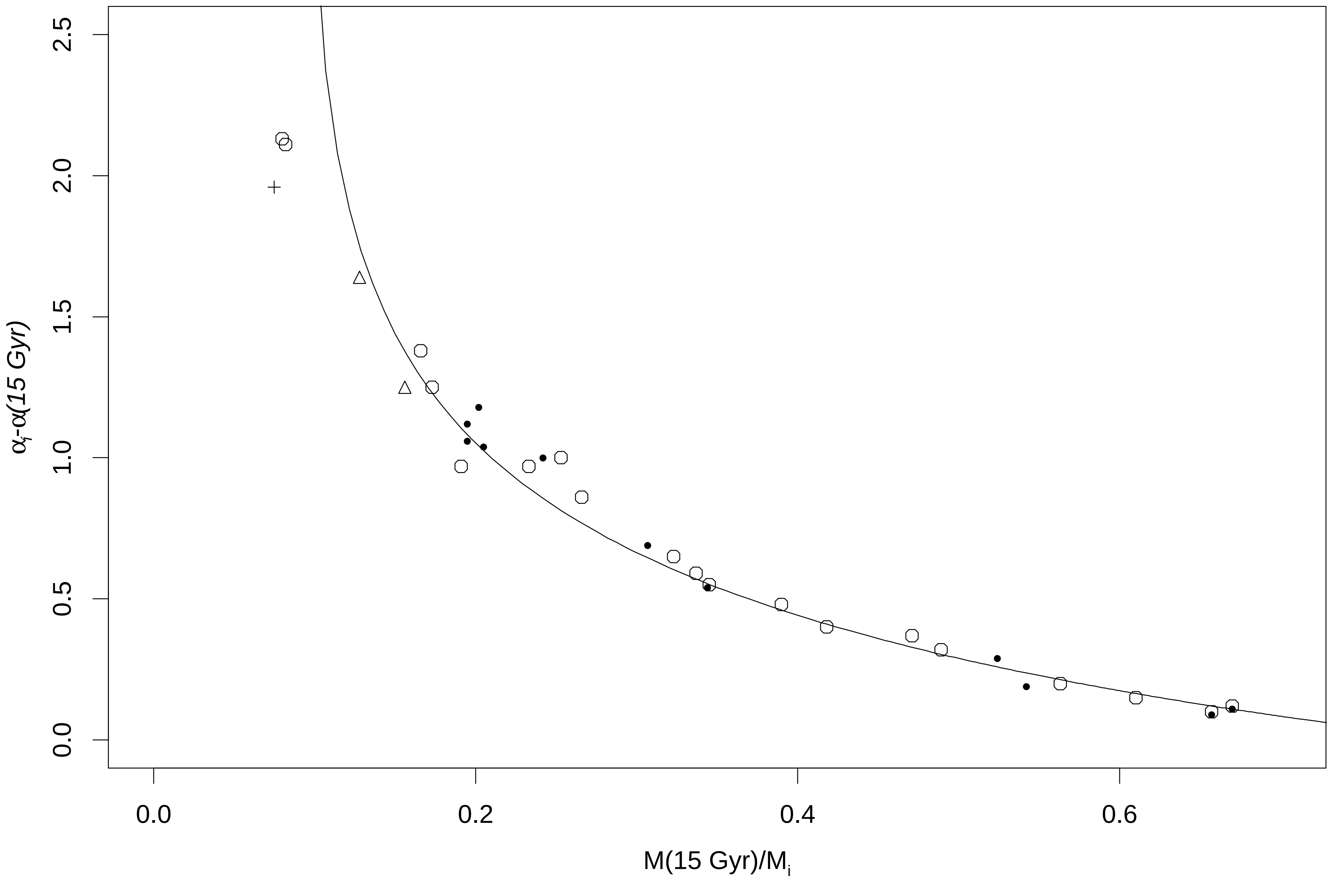

2.5
2.0
1.5
1.0
0.5
0.0
α_i-α(15 Gyr)
0.0
0.2
0.4
0.6
M(15 Gyr)/M_i

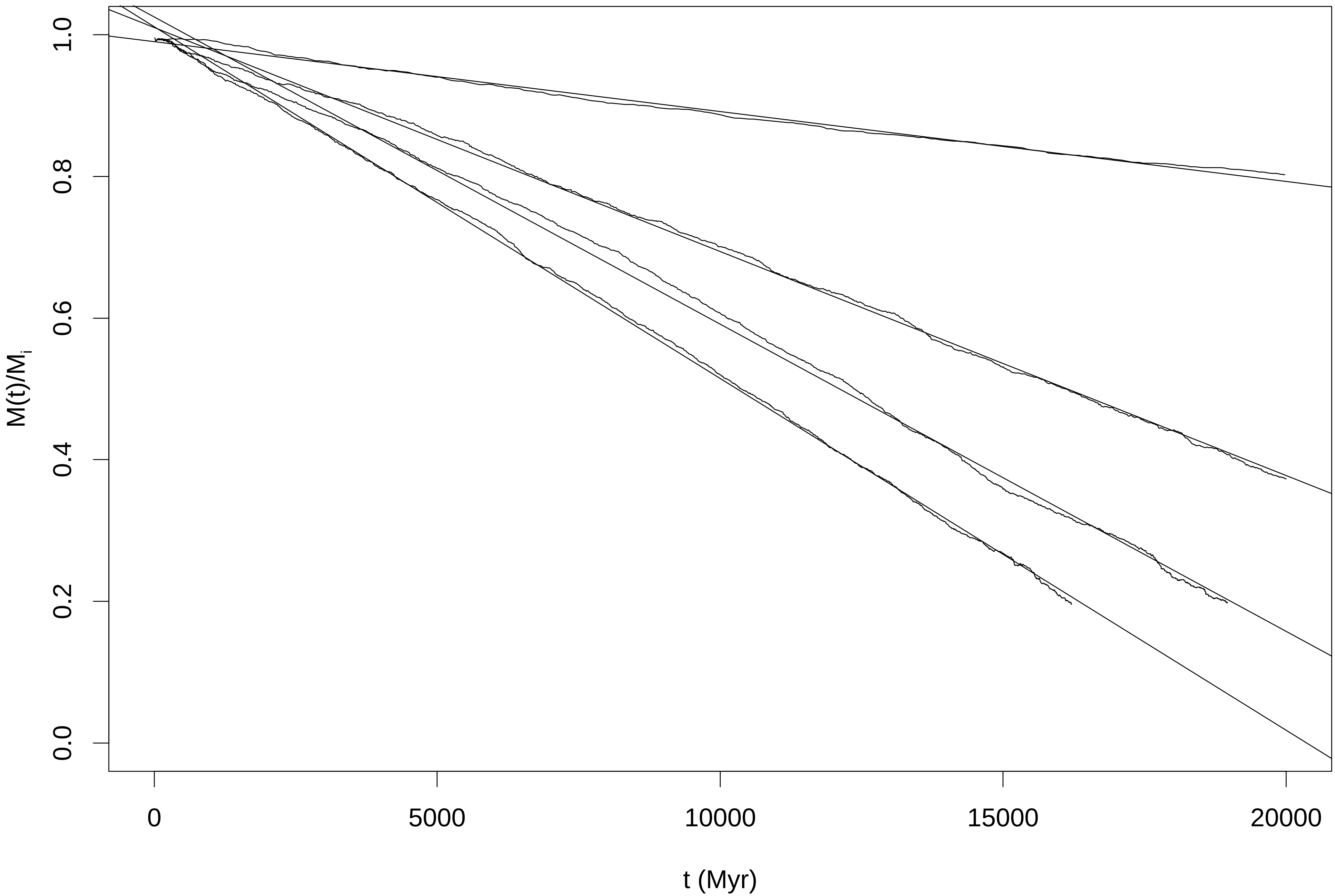

M(t)/M$_i$
0.0
0.2
0.4
0.6
0.8
1.0
0
5000
10000
15000
20000
t (Myr)

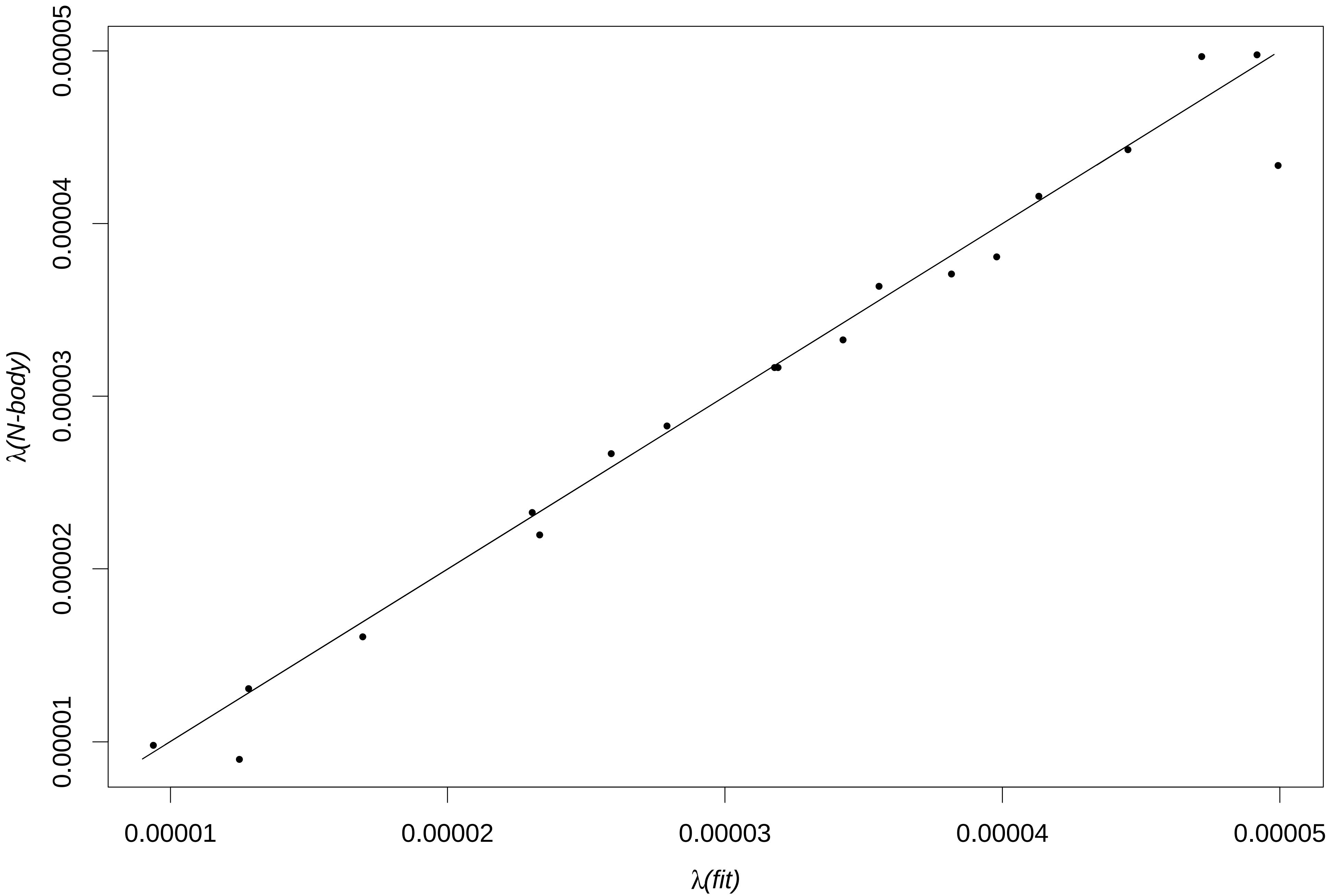
0.00001
0.00002
0.00003
0.00004
0.00005
λ(fit)
0.00001
0.00002
0.00003
0.00004
0.00005
λ(N-body)

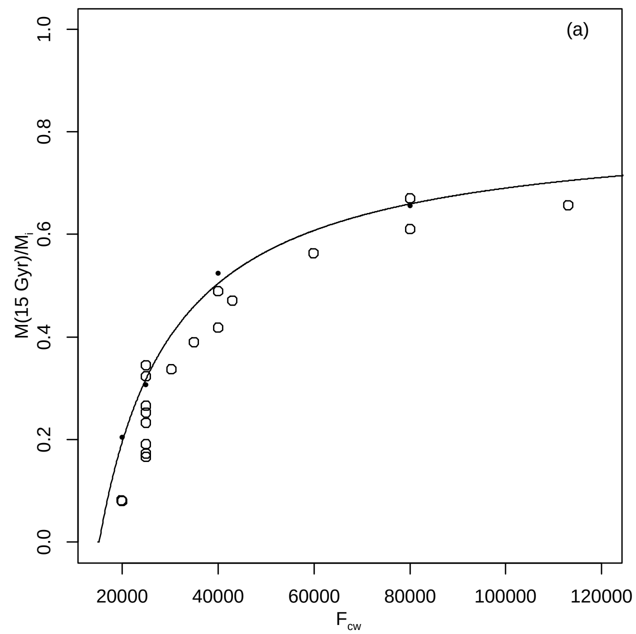

(a)
M(15 Gyr)/M_i
0.0
0.2
0.4
0.6
0.8
1.0
20000
40000
60000
80000
100000
120000
F_cw

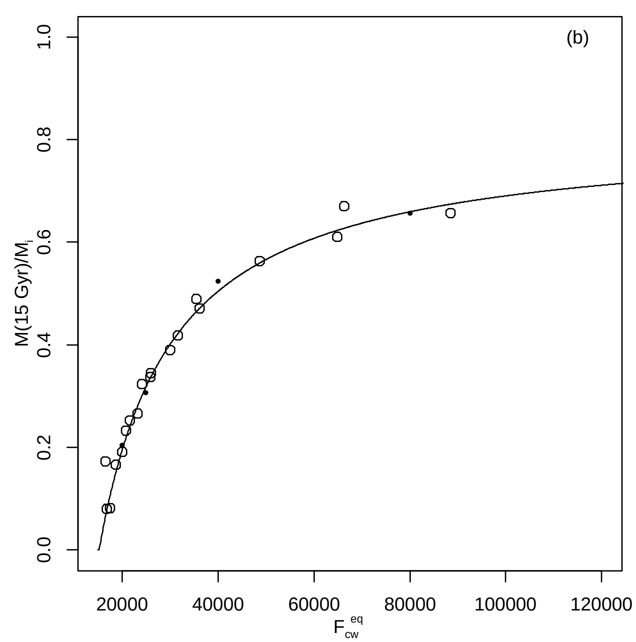

(b)
M(15 Gyr)/M_i
0.0
0.2
0.4
0.6
0.8
1.0
20000
40000
60000
80000
100000
120000
F_cw^eq

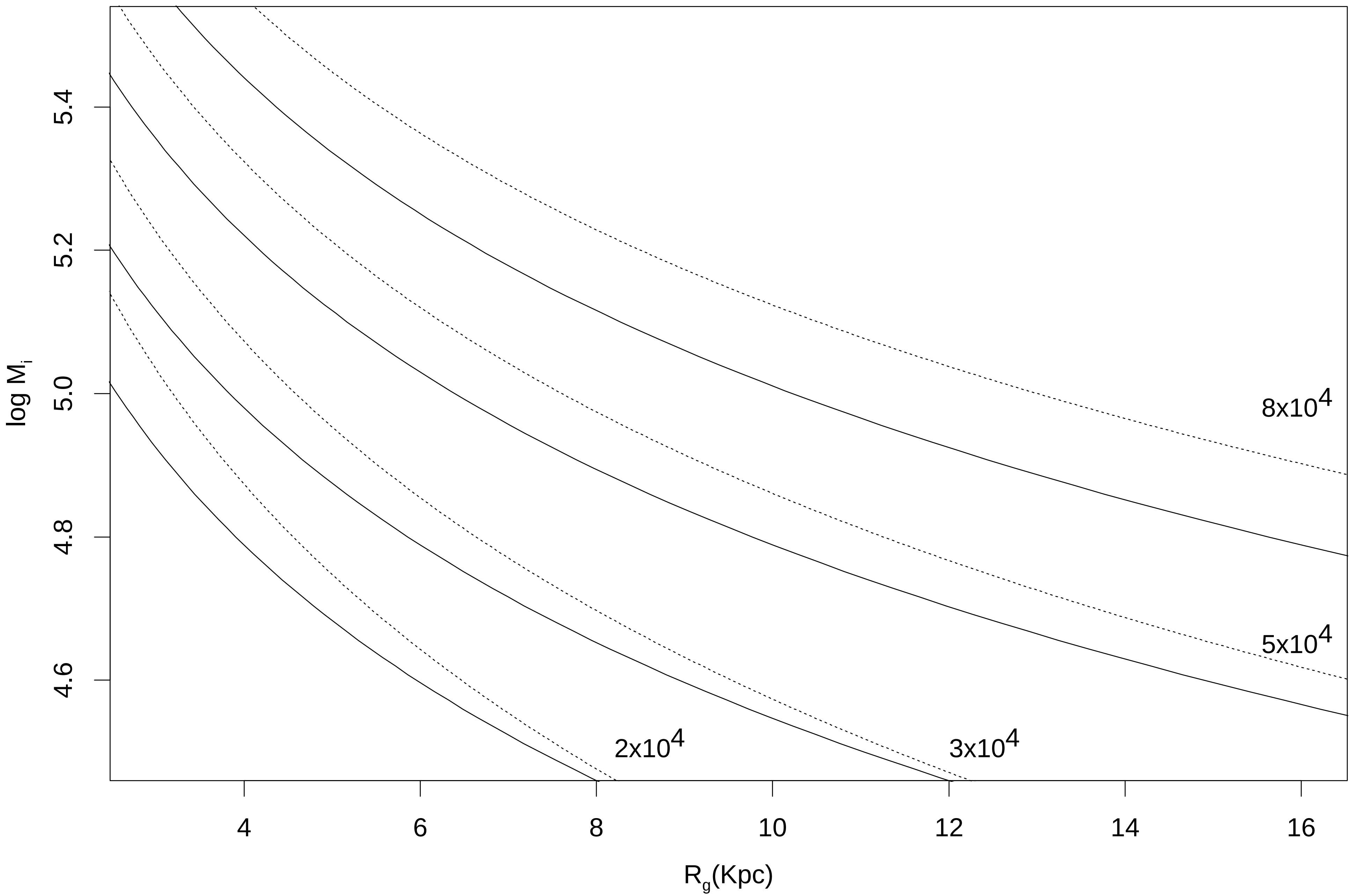
log M_i
5.4
5.2
5.0
4.8
4.6
4
6
8
10
12
14
16
R_g(Kpc)
$8x10^4$
$5x10^4$
$2x10^4$
$3x10^4$

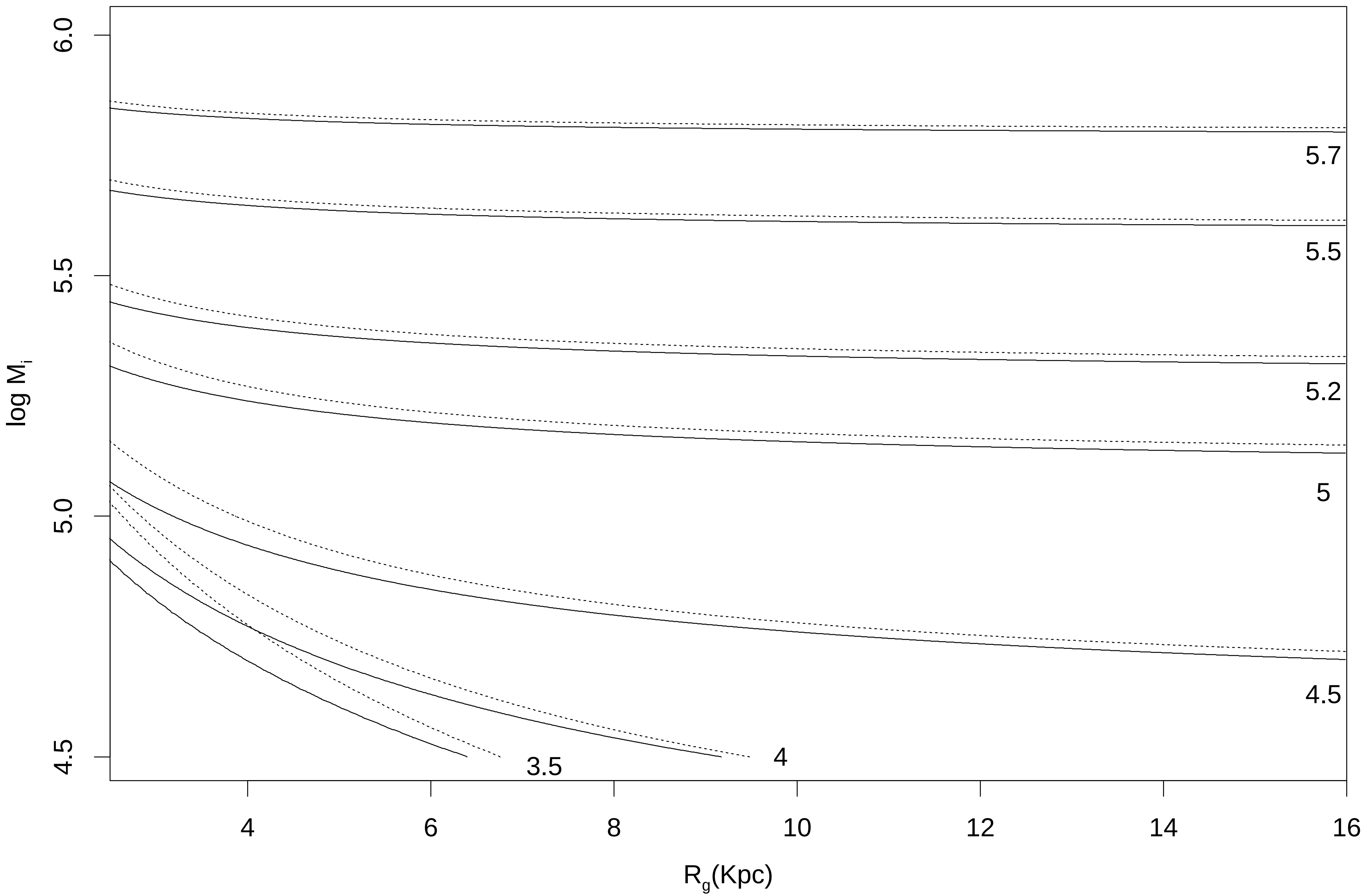

6.0
5.5
5.0
4.5
log M_i
4
6
8
10
12
14
16
R_g(Kpc)
5.7
5.5
5.2
5
4.5
4
3.5

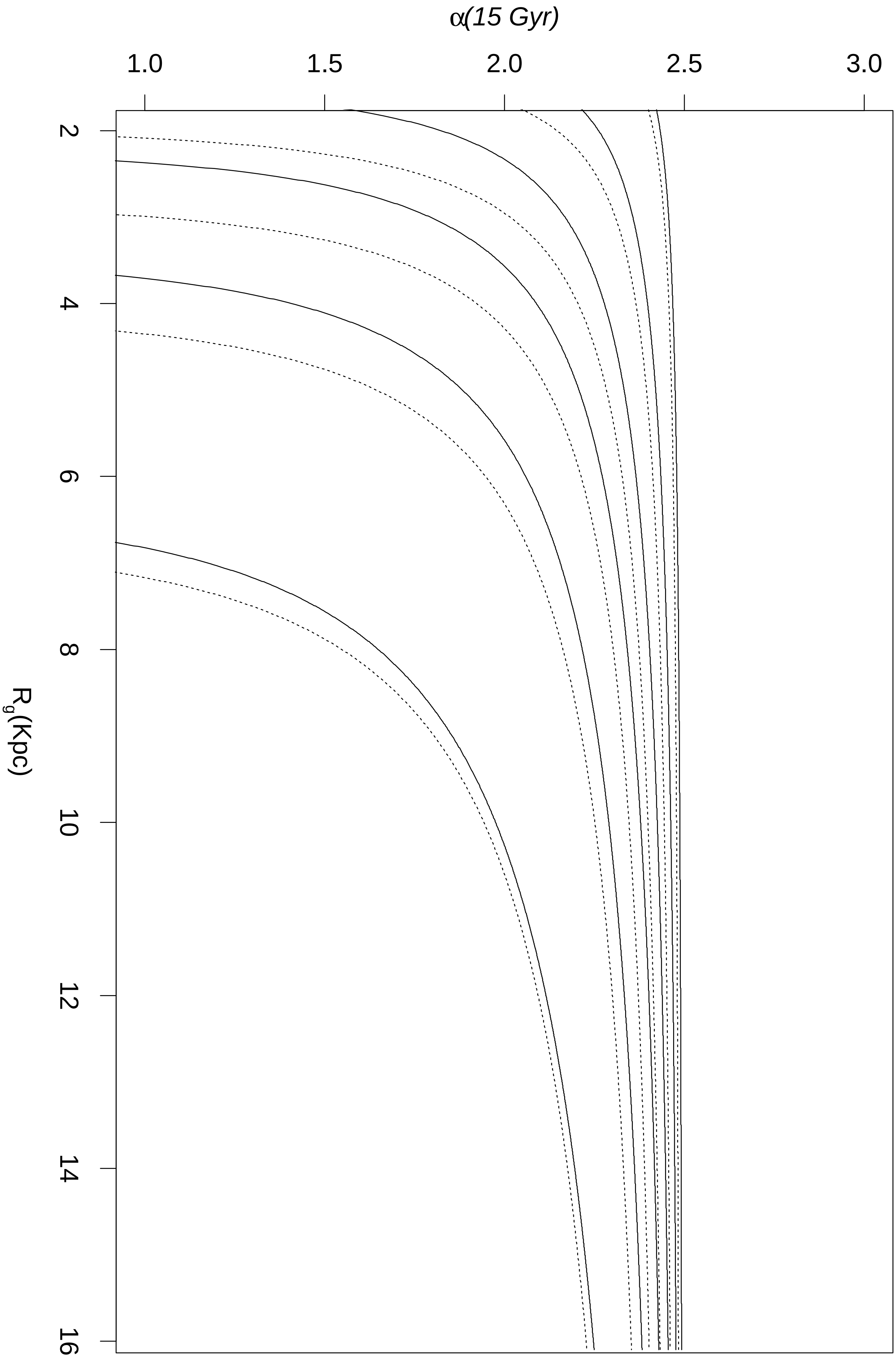

α(15 Gyr)
1.0
1.5
2.0
2.5
3.0
2
4
6
8
10
12
14
16
R_g(Kpc)

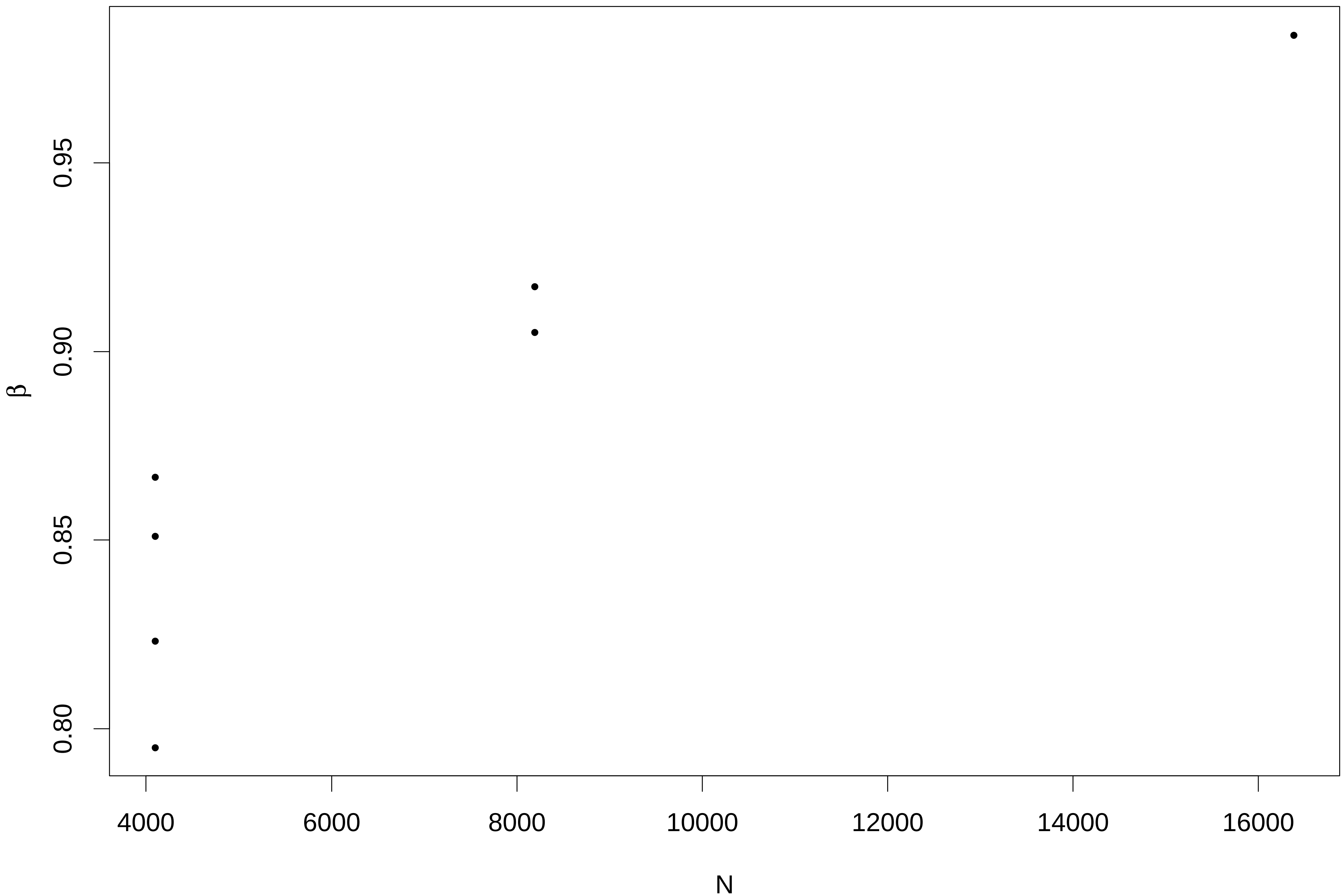

β
0.80
0.85
0.90
0.95
4000
6000
8000
10000
12000
14000
16000
N